Authors' final (accepted) version
Published as: Plasma Phys. Control. Fusion 63, 085017, 2021
https://doi.org/10.1088/1361-6587/ac0a3c

Physics of Turbulence Spreading and Explicit Nonlocality

Qinghao Yan[1,2,*] and P. H. Diamond[3,1,†]

[1] *Center for Fusion Sciences, Southwestern Institute of Physics, Chengdu, Sichuan 610041, People's Republic of China*

[2] *Department of Engineering Physics, Tsinghua University, Beijing 100084, People's Republic of China*

[3] *Center for Astrophysics and Space Sciences (CASS) and Department of Physics, University of California San Diego, La Jolla, California 92093, USA*

Abstract

In this paper, we systematically derive a model for turbulence spreading from the basic kinetic equation. The model contains explicit nonlocal nonlinear diffusion and nonlocal growth. When the nonlocality scale parameter δ_b (banana width) vanishes, this model reduces to the usual turbulence spreading model. We elucidate the mechanisms of nonlinear saturation and nonlocal growth. Results show that nonlocal effects, especially the nonlocal growth, thicken the turbulence spreading front and increase the speed of front propagation. More turbulence intensity penetrates the stable region when δ_b increases. The penetration depth Δ_p is proportional to δ_b/L_T, therefore the fraction of turbulence in the unstable region scales as $1-\delta_{b*}$. The transport scales the same way.

Keywords: turbulence spreading, explicit nonlocality, transport scaling

* qinghaoyan@outlook.com

† pdiamond@ucsd.edu

I. INTRODUCTION

Confinement and anomalous transport remain of critical concern to magnetic confinement. Indeed, plans for ignition in ITER are based upon extrapolation of present-day enhanced confinement regimes, such as H-mode [1]. Turbulent transport theory and modelling have been developed from the idea that a local mixing precess is at work, and that local fluxes may be expressed in (generalized) proportionality to local gradient. Pioneered by Boris B. Kadomtsev in his seminal work of 1965 [2], this concept of transport - as local-gradient-driven mixing - is based upon the presumption that two disparate scales control the transport. These are, of course, the mode width scale (radial correlation length Δr_c) and the profile scale (L_P, L_T, $L_n \cdots$). The correlation length is $\Delta r_c \simeq \alpha \rho_i$, where ρ_i is ion gyro radius and α is of order a few. Then the fundamental ordering is $\Delta r_c / L_n \sim \rho_* \ll 1$, where $\rho_* \sim \rho_i / L_\perp \sim \rho / a$. As a consequence, the transport scaling for drift wave microturbulence is then $D_{\rm GB} \sim \rho_* D_{\rm B}$, where $D_{\rm B} \simeq \rho_{\rm i} C_{\rm S}$ corresponds to Bohm diffusion, $C_{\rm S}$ is sound velocity and $D_{\rm GB}$ refers to Gyro-Bohm. Of course, Gyro-Bohm scaling is optimistic, because it predicts that "bigger is better", i.e. $D_{\rm GB}$ drops with increasing device size. This approach to transport modelling has culminated in what might be called the "standard model" of drift wave-zonal flow turbulence [3]. In this model, mesoscales help regulate transport via the effects of zonal flow shearing upon eddy size, but are assumed not to contribute directly to transport itself.

However, things are not so simple. Breaking of Gyro-Bohm scaling has been observed [4, 5], with $D_{\rm eff} \sim \rho_*^\sigma D_{\rm B}$, $\sigma < 1$. Moreover, a host of "non-local transport experiments", reviewed in reference [6], highlight puzzling phenomena where one part of the plasma responds rapidly to a perturbation in the other. Typical of these is the well know experiment of Gentle et al. [7], in which a rapid rise in core temperature is observed in response to edge cooling. Ongoing work continues the study of these "non-local phenomena" [8].

Theory has responded to these challenges by developing models which loosen the heretofore tight coupling of the fluctuations and fluxes to local gradients. One example of this sort of extension is "turbulence spreading" or "entrainment" [9–11], in which turbulence propagates dynamically. Another is avalanching [12, 13], whereby correlated local overturning or mixing events cooperate to produce a transport pulse and turbulence burst. These mechanisms are reviewed in depth in Ref. [14]. The upshot is a basis for understanding how

fast propagation of turbulence and transport fronts can occur. These ideas are encapsulated in transport modelling by replacing the traditional Fick's law, say of the form $Q = -\chi \nabla T$, with a delocalized flux-gradient relation $Q = -\int \mathrm{d}r' K(r - r')\nabla T(r')$ [15, 16]. Of course, here the structure and range of the kernel $K(r - r')$ are the key issues.

All of this, then, motivates the question of whether or not the transport dynamics is explicitly non-local, or simply local, but exhibiting fast front propagation. By explicit non-local, we mean say, the evolution of fluctuating potential intensity $\langle\tilde{\phi}^2\rangle$ of the form $\partial_t\langle\tilde{\phi}^2\rangle = \int \gamma(r - r')\langle\tilde{\phi}^2\rangle(r')\mathrm{d}r' + \cdots$ as opposed to the usual form:

$$\partial_t \mathcal{E} = \partial_x[(D_0\mathcal{E})\partial_x\mathcal{E}] + \gamma(x)\mathcal{E} - \sigma\mathcal{E}^2 \tag{1}$$

for fluctuation energy evolution, familiar from $K - \varepsilon$ modelling. If nonlocality is explicit, then the range of kernel is of prime importance. Of course, it is also critical to understand exactly how such explicit nonlocality can result from a system of basic equations which are local partial differential equations.

In this paper, we answer the question above in the *affirmative*. Yes - the equation for potential fluctuation intensity $\langle\tilde{\phi}^2\rangle$ is *explicitly* non-local. Note that:

1. in the sense of a quasi-linear approximation, all transport fluxes may be calculated from the knowledge of the intensity $\langle\tilde{\phi}^2\rangle$;

2. such a result is equivalent to stating that the dynamics of turbulence spreading is explicitly non-local.

Here, the fundamental system is the Darmet model of trapped ion turbulence [17–19], governed by a function $f(\psi, \alpha, E, t)$ of a two space coordinates (ψ, α) and energy E distribution. This evolves in time according to a gyro-kinetic equation, as well as the quasi-neutrality condition, including polarization charge. The scale variation of the modes should not smaller than the banana width. Thus, it is not surprising that the scale of explicit nonlocality is the banana width δ_b in radial direction. Here $\delta_b \simeq \sqrt{R/r}q\rho_i$, and R is major radius, q is the safety factor. Thus, we see that the nonlocality, while physical, is rather modest. This is in accord with current expectations. We have serval reasons for choosing trapped ion turbulence as the representative. First, this model is closely analogous to the gyro-kinetic system, and is simple model manifesting ITG turbulence. Growth can be included easily via the drift velocity. At the same time, this (Darmet trapped ion turbulence) model is simple. Since,

only bounce averaged quantities are evolved, it requires only 2 spatial dimensions. And since precession frequency is parameterized by energy, only one velocity space variable is needed. Thus the model reduce the space from 5D, as for standard gyro-kinetics, to 3D. Second, in the original calculation of zonal flow from Rosenbluth and Hinton [20], they identified the trapped ion enhanced polarization charges as the effect, which sets ZF screening. Thus a model based on trapped ion is a good way to treat both zonal flow and turbulence spreading. This is our ultimate goal. As for the relevance to future tokamak, first, this model can be a baseline for calculation of turbulence spreading – it clarifies physical concepts and ideas. Second, when the temperature of ion increases, the normalized collision frequency ν_{*i} drops, thus the trapped particle effects can be enhanced.

The analysis undertaken in this paper may be summarized as follows. The fundamental scale ordering is:

$$\rho_i < \delta_b < l_s < L_T, \text{ and } \rho_i < l_r < l_s$$

where:

- ρ_i, ion gyro radius,
- $\delta_b \simeq \sqrt{R/r} q \rho_i$, ion banana orbit width,
- $1/l_r \equiv k_r$, the scale of the mode, which is comparable to the correlation length Δr_c,
- $1/l_s \equiv \partial_r |\phi|^2/|\phi|^2$, l_s is spectral variation scale. Spectral variation l_s is the scale of the spectral envelope, which is formed by the intensity profile of modes of $\tilde{\phi}$, therefore larger or equal to the scale l_r. The scaling l_s can be expected to be $l_s \sim \delta_b^\alpha L_{T_i}^\beta$, where $\alpha < 1, \beta < 1, \alpha + \beta = 1$. l_s is set by profiles and the zonal flow screening (hence δ_b dependence).
- $1/L_{T_i} \equiv \partial_r \langle T_i \rangle / \langle T_i \rangle$, L_{T_i} or L_T is a scale of the constant-temperature-gradient region which is of the same order as the box size.

Exploiting the scale ordering, we proceed from the basic gyro-kinetic equation to obtain a potential vorticity (PV) evolution equation and then the equation for the evolution of the PV correlation function $\langle \tilde{U}(1)\tilde{U}(2) \rangle$, where $\tilde{U}(1)$ and $\tilde{U}(2)$ indicate the potential vorticity at different positions. The correlation equation is closed by a two-point quasilinear method.

A key step comes when inverting $\langle \tilde{U}(1)\tilde{U}(2)\rangle$ to obtain $\langle \tilde{\phi}(1)\tilde{\phi}(2)\rangle$. The inversion is accomplished by the use of a Green's function. with kernel scale δ_b. This ultimately defines the scale of explicit non-locality in the problem. Note the important physics findings that:

1. the theory of spreading is most "naturally" formulated in terms of a conserved charge density, or PV;

2. the scale of PV inversion - i.e. the transformation $\tilde{U} \to \tilde{\phi}$ - defines the scale of explicit non-locality in the transport flux.

We derive the equation for $\langle \tilde{\phi}^2 \rangle$ and discuss the physics of turbulence spreading. The key novel effect here is that of non-local growth. We show how non-local growth enhances the speed of the spreading front, the penetration of stable regions by turbulence spreading, and how such enhanced spreading contributes to nonlinear saturation. Extensions of this work to other systems and problems are discussed.

The remainder of this paper is organized as follows. Section II presents the evolution equations for fluctuating temperature and potential. Section III studies the spectral evolution equation. Section III A presents the evolution equation of turbulence enstrophy. Section III B gives the evolution equation of potential intensity form turbulence enstrophy. Numerical analysis of modified intensity evolution are presented in section IV. Section V gives conclusions and discussions.

II. FROM KINETICS TO PV DYNAMICS

The distribution function $f(\mathbf{x}, \mathbf{p}, t)$ is a function of phase space $(\mathbf{x}, \mathbf{p})$, which can be replaced by a set of action-angle variables $(\mathbf{J}, \phi)$. For trapped ions, $\mathbf{J} = (J_1, J_2, J_3)$, which are adiabatic invariants. (ϕ_1, ϕ_2, ϕ_3) are gyro phase, bounce phase and precession phase. For the study of low frequency ($\omega < \omega_b$, ω_b is the typical bounce frequency of ion) turbulence in a tokamak, a double averaged (on both gyro phase and bounce phase) distribution function $\bar{f}$ can be used to simplify the phase space to 3D (ψ, α, E). Here ψ and α are the radial and angle coordinates, and E is the energy or velocity coordinate. The averaging is done in both gyro-phase and bounce-phase. $\bar{f}$ is determined by the kinetic equation[17]:

$$\partial_t \bar{f} + \Omega_D E \partial_\alpha \bar{f} - [J_0\phi, \bar{f}] = 0 \tag{2}$$

where $[F, G] = \partial_\alpha F \partial_\psi G - \partial_\psi F \partial_\alpha G$, and J_0 is a gyro- and bounce-averaging operator. Here Ω_D is the precession frequency of trapped particles, assumed to be constant.The time scale is in units of a typical precession time, since the kinetic equation is averaged over the bounce phase. Because the length scale of trapped ion turbulence is of the order of banana width (which is vastly exceeds the Debye length), the Poisson equation is replaced by quasi-neutrality constraint $n_i = n_e$.

We can decompose the distribution function $\bar{f}$ into a mean distribution $\langle f \rangle$, the adiabatic response function $-\langle f \rangle q_{i,e}\phi/T_{i,e}$, and the non-adiabatic part $h_{i,e}$. An important point is that the fluctuating particle density should not respond to the zonal mode, i.e. the adiabatic fluctuation only responds to the non-zonal potential. Then the adiabatic distribution function changes to $-\langle f \rangle q_{i,e}(\phi - \phi_Z)/T_{i,e}$. Here $\phi_Z \equiv \langle \phi \rangle_\alpha$ is the zonal potential. And after integration of this distribution function in velocity (energy) space, we obtain $\widetilde{n}_{i,e}/n_0 = -q_{i,e}(\phi - \phi_Z)/T_{i,e}$. Thus we have the total distribution function below:

$$\bar{f}_{i,e} = \langle f_{i,e} \rangle - \frac{q_{i,e}}{T_{i,e}}(\phi - \phi_Z)\langle f_{i,e} \rangle + h_{i,e} \tag{3}$$

The quasi-neutrality condition $n_i = n_e$ now can be represented by the integral of total distribution function in the velocity (energy) space as below:

$$\begin{aligned} &\frac{2}{n_0\sqrt{\pi}} \int_0^\infty J_0 \left[-\frac{q}{T_i}(\phi - \phi_Z)\langle f_i \rangle + h_i \right] \sqrt{E} \mathrm{d}E + \overline{\Delta}_i \frac{q\phi}{T_i} \\ &= \frac{2}{n_0\sqrt{\pi}} \int_0^\infty J_0 \left[\frac{q}{T_e}(\phi - \phi_Z)\langle f_e \rangle + h_e \right] \sqrt{E} \mathrm{d}E - \overline{\Delta}_e \frac{q\phi}{T_e} \end{aligned} \tag{4}$$

$\overline{\Delta}_s = \rho_{0s}^2 \partial_\alpha^2 + \delta_{bs}^2 \partial_\psi^2$ accounts for the polarization - i.e. the difference between the density of bounce-averaged centers and the density of particles. Equation (4) could be included in equation (6), a kinetic quasi-neutrality equation, whose R.H.S. is determined by the non-adiabatic particle distribution function $h_{i,e}$, and thus by non-adiabatic charges $\widetilde{n}_{\mathrm{nonad},i}$ and $\widetilde{n}_{\mathrm{nonad},e}$. Meanwhile, the non-adiabatic distribution function satisfies the kinetic equation

(5) below.

$$\begin{aligned}
&\partial_t h_i + \Omega_D E \partial_\alpha h_i - \left[\bar{\phi}, -\frac{q}{T_i}(\phi-\phi_Z)\langle f_i\rangle + h_i\right] \\
&\quad = \partial_t\left(\frac{q}{T_i}(\phi-\phi_Z)\langle f_i\rangle\right) + \partial_\alpha(\overline{\phi-\phi_Z})\partial_\psi\langle f_i\rangle
\end{aligned} \tag{5}$$

$$\begin{aligned}
&C_{ad}\,(\phi-\phi_Z) - C_i\overline{\Delta}_{i+e}\phi \\
&\quad = \frac{2}{n_0\sqrt{\pi}}\left(\int_0^\infty J_0 h_i\sqrt{E}\mathrm{d}E - \int_0^\infty J_0 h_e\sqrt{E}\mathrm{d}E\right) \\
&\quad = \widetilde{n}_{\mathrm{nonad},i} - \widetilde{n}_{\mathrm{nonad},e}
\end{aligned} \tag{6}$$

Here $C_i = q/T_i$, $C_{ad} = C_i(1+\tau)/\sqrt{2\varepsilon_0}$, $\tau = T_i/T_e$, $\overline{\Delta}_{i+e} = \overline{\Delta}_i + \tau\overline{\Delta}_e$. $(\overline{\phi-\phi_Z})$ represents the double-phase-averaged potential. $\varepsilon_0 = a/R$ is the inverse aspect ratio, and $\sqrt{2\varepsilon_0}$ is the fraction of trapped particles. Equations (5) and (6) are used in reduced gyro-kinetic simulation of trapped ion modes [17–19]. For the kinetic quasi-neutrality equation (6), we assume adiabatic electrons, i.e. $h_e = 0$, and neglect the $\overline{\Delta}_e$ term. Taking the derivative of equation (6) with respect to time, we obtain $\partial_t h_i$ in the R.H.S. Using equation (5) to eliminate $\partial_t h_i$, and doing the energy integral $(2/n_0\sqrt{\pi})\int_0^\infty ...\sqrt{E}\mathrm{d}E$ yields,

$$\begin{aligned}
&\partial_t\left[C_e(\phi-\phi_Z) - C_i\overline{\Delta}_i\phi\right] = \\
&\quad -\frac{3}{2}\Omega_D\partial_\alpha\widetilde{T}_i + \left[\phi, -\frac{q}{\sqrt{2\varepsilon_0}T_i}(\phi-\phi_Z) + \frac{\widetilde{n}_i}{n_0}\right] \\
&\quad -\frac{1}{\sqrt{2\varepsilon_0}}\widetilde{v}(\psi)\partial_\psi\ln\langle n_i\rangle
\end{aligned} \tag{7}$$

where part of C_{ad} is cancelled and left $C_e = C_i\tau/\sqrt{2\varepsilon_0}$, and we simply take $J_0\phi = \bar{\phi} = \phi$. When doing the integral of $\langle f_i\rangle$, we encounter $1/\sqrt{2\varepsilon_0}$, because $\langle f_i\rangle$ is the distribution function of all particles, including both passing and trapped particles. We want to separate the evolution of the zonal mode ($\phi_Z \equiv \langle\phi\rangle_\alpha$) from ϕ. So we write $\phi = \widetilde{\phi} + \phi_Z$, where $\widetilde{\phi}$ are the $n \neq 0$ trapped ion modes. Substituting all ϕ into the equation above, and replacing $\tilde{n}_i$ with equation (6), we can separate the results into two equations according to symmetry[21–23], as below. The subscript i in $\overline{\Delta}_i$ is neglected.

$$\begin{aligned}
&\left(\frac{\partial}{\partial t} + \widetilde{\mathbf{v}}\cdot\nabla + \mathbf{V}_Z\cdot\nabla\right)(C_i\overline{\Delta}\widetilde{\phi}) = \frac{3}{2}\Omega_D\partial_\alpha\widetilde{T}_i \\
&\qquad -iC_e(\omega-\omega_Z+\frac{\omega^i_{*n}}{\tau})\widetilde{\phi} - C_i\tilde{v}(\psi)\partial_\psi(\overline{\Delta}\phi_Z)
\end{aligned} \tag{8}$$

$$\begin{aligned}
\frac{\partial}{\partial t}\left(C_i\overline{\Delta}\phi_Z\right) &= C_i\langle\nabla\widetilde{\phi}\times\hat{z}\cdot(\nabla\overline{\Delta}\widetilde{\phi})\rangle_\alpha \\
&\equiv -C_i\delta_{b0}^2\partial_\psi^2\left\langle\tilde{v}_\psi\tilde{v}_\alpha\right\rangle_\alpha
\end{aligned} \tag{9}$$

where $\widetilde{\mathbf{v}} = -\nabla\widetilde{\phi}\times\hat{z}$, $\mathbf{V}_Z = -\nabla\phi_Z\times\hat{z} = \partial_\psi\phi_Z\hat{\mathbf{e}}_\alpha$. The Doppler shift effect terms are $\omega^i_{*n} = \frac{k_\alpha cT}{qB}\partial_\psi \ln\langle n_i\rangle$, $\omega^i_{*T} = \frac{k_\alpha cT}{qB}\partial_\psi \ln\langle T_i\rangle$, $\omega_Z = k_\alpha\frac{\partial\phi_Z}{\partial\psi}$. When the zonally averaged profiles $\langle T\rangle$ and $\langle n\rangle$ exhibit no corrugations, as shown in figure 1, we set $L_n^{-1}\equiv\partial_\psi\ln\langle n_i\rangle > 0$ and $L_T^{-1}\equiv\partial_\psi\ln\langle T_i\rangle > 0$. Equations (8) and (9) are the evolution equations for vorticity. In equation (8), the second term on the R.H.S can be combined with the L.H.S., yielding a useful evolution equation for potential vorticity $(\tilde{\phi}-\overline{\Delta}\tilde{\phi})$. Equation (9) shows that zonal vorticity evolves according to Reynolds force, as expected.

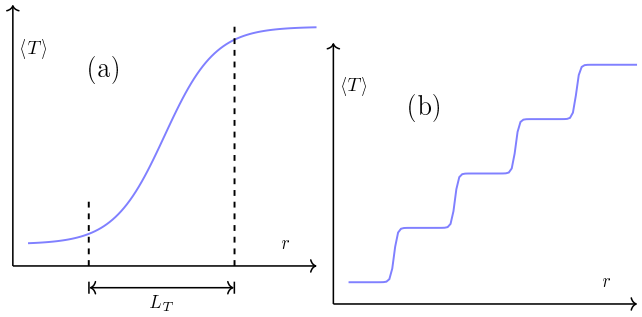

FIG. 1. The characteristic length scale L_T of mean profile is defined in (a). For a corrugated profile like (b), no appropriate L_T could be defined

We notice the first term on the R.H.S. of (8) contains the fluctuating temperature $\tilde{T}_i$. We can substitute the full $\bar{f}_i$ and ϕ into the kinetic equation (5), and then obtain the fluctuating temperature $\tilde{T}_i$ evolution by taking the energy moment, i.e. $\frac{2}{3}\frac{2}{n_0\sqrt{\pi}}\int_0^\infty ...E\sqrt{E}\mathrm{d}E$. Then separating the result according to symmetry yields:

$$\begin{aligned}\sqrt{2\varepsilon_0}\left(\partial_t+\widetilde{\mathbf{v}}\cdot\nabla+\mathbf{V}_Z\cdot\nabla\right)\widetilde{T}_i \\ = -i(\omega-\omega_Z-\omega^i_{*n}-\omega^i_{*T})\langle T_i\rangle\frac{q\widetilde{\phi}}{T_i}\end{aligned} \tag{10}$$

$$\begin{aligned}\frac{\partial}{\partial t}\left(\langle T_i\rangle+\langle T_i\rangle\ln\langle n_i\rangle\right) = \sqrt{2\varepsilon_0}\langle\nabla\widetilde{\phi}\times\hat{z}\cdot\nabla\widetilde{T}_i\rangle_\alpha \\ \equiv -\sqrt{2\varepsilon_0}\partial_\psi\langle\widetilde{v}_\psi\widetilde{T}_i\rangle_\alpha\end{aligned} \tag{11}$$

We study turbulence evolution by using equations (8) and (10). Notice the similarity between (8) and (10)-they can be written into a simpler way. First, multiply the above equations (10) and (11) by $\tau/(\sqrt{2\varepsilon_0}\langle T_i\rangle)$. Then subtract the two vorticity equations (8) and (9) from them. We neglect ω^i_{*n} and $\ln\langle n_i\rangle$ by assuming large L_n and slow variation of mean density. In other words, the mean density gradient is neglected in our model. Finally, we

have:

$$\frac{\partial}{\partial t}\left(\frac{\tau}{\sqrt{2\varepsilon_0}}\ln\langle T_i\rangle - C_i\overline{\Delta}\phi_Z\right) = \left\langle \nabla\widetilde{\phi}\times\hat{z}\cdot\nabla\left(\frac{\tau}{\langle T_i\rangle}\nabla\widetilde{T}_i - C_i\overline{\Delta}\widetilde{\phi}\right)\right\rangle_\alpha \tag{12}$$

$$\frac{\mathrm{d}}{\mathrm{d}t}\left(\tau\frac{\widetilde{T}_i}{\langle T_i\rangle} - C_i\overline{\Delta}\widetilde{\phi}\right) = -\frac{3}{2}\Omega_D\partial_\alpha\widetilde{T}_i - \widetilde{\mathbf{v}}\cdot\nabla\left(\frac{\tau}{\sqrt{2\varepsilon_0}}\ln\langle T_i\rangle - C_i\overline{\Delta}\phi_Z\right) \tag{13}$$

These can be written as evolution equations for mean and fluctuating potential vorticity.

$$\partial_t\langle q\rangle = \left\langle\nabla\widetilde{\phi}\times\hat{z}\cdot\nabla\delta q\right\rangle_\alpha = -\partial_\psi\left\langle\tilde{v}_\psi\delta q\right\rangle_\alpha \tag{14}$$

$$\frac{\mathrm{d}}{\mathrm{d}t}\delta q = -\frac{3}{2}\Omega_D\partial_\alpha\widetilde{T}_i - \widetilde{\mathbf{v}}\cdot\nabla\langle q\rangle \tag{15}$$

where:

$$\frac{\mathrm{d}}{\mathrm{d}t} = \frac{\partial}{\partial t} + \widetilde{\mathbf{v}}\cdot\nabla + \mathbf{V}_Z\cdot\nabla$$

The total potential vorticity $\langle q\rangle + \delta q$ is defined as,

$$\langle q\rangle = \frac{\tau}{\sqrt{2\varepsilon_0}}\ln\langle T_i\rangle - C_i\overline{\Delta}\phi_Z \tag{16}$$

$$\delta q = \tau\frac{\widetilde{T}_i}{\langle T_i\rangle} - C_i\overline{\Delta}\widetilde{\phi} \tag{17}$$

There are several interesting observations concerning the above equations (14) and (15). The total potential vorticity is conserved, up to curvature drift effects. The evolution of PV is determined by PV flux, which results from both heat flux and Reynolds stress. Theoretically, we can obtain the mean profile evolution if we know the heat flux and Reynolds stress. This requires us to obtain the explicit equations for $\tilde{\phi}$ and $\tilde{T}$. Considering the conservative form of equation (8), we will use the 2-point correlation function [24, 25] and equation (8) to obtain the turbulence intensity (i.e. $\langle\tilde{\phi}^2\rangle$) evolution equation. And as we will show in this paper, the coupling to $\tilde{T}$ in equation (8) can be decoupled by a simple quasilinear type approximation. We will then use the $\langle\tilde{\phi}^2\rangle$ equation to study turbulence spreading. The aim is to develop a generic spreading model.

III. FROM PV DYNAMICS TO SPACE-TIME SPECTRAL EVOLUTION

We defined a potential-vorticity quantity $\tilde{U} = C_e\tilde{\phi} - C_i\overline{\Delta}\tilde{\phi}$, which allow us to write the equation (8) as below, where $(\psi,\alpha)\to\vec{x}\equiv(r,y)$. We used incompressibility of fluid motion

and ignored the averaged density gradient, so:

$$\begin{aligned}\text{Eq.(8)} \Longrightarrow \left(\frac{\partial}{\partial t}+\widetilde{\mathbf{v}}\cdot\nabla+\mathbf{V}_Z\cdot\nabla\right)\tilde{U}\\ =-\frac{3}{2}\Omega_D\partial_y\widetilde{T}_i+C_i\tilde{v}_r\partial_r(\overline{\Delta}\phi_Z)\end{aligned} \tag{18}$$

Because this is a conservation equation for $\tilde{U}$ (up to curvature drift and zonal potential), we can derive the space-time evolution equation for $\langle\tilde{\phi}^2\rangle$ from the evolution equation of $\langle\tilde{U}\tilde{U}\rangle$. Based on the definition of $\tilde{U}$, we have the Fourier component of $\tilde{\phi}$ as below:

$$\widetilde{\mathcal{U}}_{\bar{k}}=(C_e+C_i\bar{k}^2)\tilde{\phi}_{\bar{k}}\longrightarrow\tilde{\phi}_{\bar{k}}=\frac{\widetilde{\mathcal{U}}_{\bar{k}}}{C_e+C_i\bar{k}^2} \tag{19}$$

which after inverse Fourier transform yields,

$$\tilde{\phi}=\int G(x,x')\tilde{U}(x')\mathrm{d}x'$$

$\langle\tilde{\phi}_1\tilde{\phi}_2\rangle$ follows naturally from applying the Green's functions to the two-point PV correlation function $\langle\tilde{U}(1)\tilde{U}(2)\rangle$ (or written as $\langle\tilde{U}_1\tilde{U}_2\rangle$). Then the limit of $1\to2$ gives $\langle\tilde{\phi}^2\rangle$:

$$\left\langle\tilde{\phi}^2\right\rangle=\lim_{1\to2}\iint G_1(x_1,x_1')G_1(x_2,x_2')\left\langle\tilde{U}(x_1')\tilde{U}(x_2')\right\rangle\mathrm{d}x_1'\mathrm{d}x_2' \tag{20}$$

$\langle\tilde{\phi}^2\rangle$ characterizes the intensity of turbulence, which can then be used to calculate transport coefficients. The limitation of $r_1\to r_2$ represents the radial distance between quantities $\tilde{\phi}_1$ and $\tilde{\phi}_2$ is less than the mode correlation scale l_r. Here we give a road map for the derivation.

1. We first obtain the evolution equation of $\langle\tilde{U}_1\tilde{U}_2\rangle$ by adding $\tilde{U}_1\partial_t\tilde{U}_2+\tilde{U}_2\partial_t\tilde{U}_1$. Nonlinear correlation terms in the evolution of $\langle\tilde{U}_1\tilde{U}_1\rangle$ can be approximated by a two-point quasi-linear response function.

2. Then applying the Green's functions to the evolution equation for $\langle\tilde{U}_1\tilde{U}_2\rangle$ yields the evolution equation for $\langle\tilde{\phi}_1\tilde{\phi}_2\rangle$. Using the property that the spectral length is larger than the convolution kernel scale, we can simplify terms like $\int G(x_1,x_1')G(x_2,x_2')T_r(x_1',x_2')\mathrm{d}x_1'\mathrm{d}x_2'$. The result will be

$$\partial_t\left\langle\tilde{\phi}_1\tilde{\phi}_2\right\rangle+\nu(1,2)\left\langle\tilde{U}_1\tilde{U}_2\right\rangle=\gamma(1,2)+\cdots$$

   Here $\nu(1,2)$ comes from Green function convolution with the flux term, and is represented by a Krook form. It involves integrals and introduces contributions which cannot be written as the divergence of a flux. $\gamma(1,2)$ also involves the Green's functions.

3. Hence finally, after taking the limit of $1 \to 2$, we get the evolution equation for $\langle\tilde{\phi}^2\rangle$. It *differs* from the oft-assumed forms [9–11]:

$$\partial_t \mathcal{E} + \nabla \cdot \Gamma_{\mathcal{E}} = \gamma_L \mathcal{E} + \cdots$$

where $\mathcal{E}$ is the turbulence energy, $\Gamma_{\mathcal{E}}$ and γ_L are determined by turbulence *only locally*.

A. Evolution equation for Potential Enstrophy

First, let's derive the evolution equation for 2-point PV correlation function $\langle\tilde{U}_1\tilde{U}_2\rangle$, $\tilde{U}_1$ is the function at point $x_1 \equiv (r_1, y_1)$. Multiplying $\tilde{U}_2$ by the evolution equation for $\tilde{U}_1$, we have

$$\begin{aligned}\tilde{U}_2\partial_t\tilde{U}_1 + \partial_{r1}(\tilde{v}_{r1}\tilde{U}_1\tilde{U}_2) + \partial_{y1}(\tilde{v}_{y1}\tilde{U}_1\tilde{U}_2) + \mathbf{V}_Z\partial_{y1}(\tilde{U}_1\tilde{U}_2)\\ = -\frac{3}{2}\Omega_D\tilde{U}_2\partial_{y1}\widetilde{T}_i(1) + C_i\tilde{U}_2\tilde{v}_r(1)\partial_r(\overline{\Delta}\phi_Z)\end{aligned} \tag{21}$$

Adding the corresponding parts from $\tilde{U}_1\partial_t\tilde{U}_2$, gives:

$$\begin{aligned}&\partial_t\left(\tilde{U}_1\tilde{U}_2\right) + \partial_{r_1}\left(\tilde{v}_{r_1}\tilde{U}_1\tilde{U}_2\right) + \partial_{r_2}\left(\tilde{v}_{r_2}\tilde{U}_1\tilde{U}_2\right)\\ &\quad + \partial_{y_1}\left(\tilde{v}_{y_1}\tilde{U}_1\tilde{U}_2\right) + \partial_{y_2}\left(\tilde{v}_{y_2}\tilde{U}_1\tilde{U}_2\right)\\ &\quad + \mathbf{V}_Z\left(\partial_{y_1} + \partial_{y_2}\right)\left(\tilde{U}_1\tilde{U}_2\right)\\ &= -\frac{3}{2}\Omega_D\left(\tilde{U}_2\partial_{y1}\widetilde{T}_i(1) + \tilde{U}_1\partial_{y2}\widetilde{T}_i(2)\right)\\ &\quad + C_i\partial_r(\overline{\Delta}\phi_Z)\left(\tilde{U}_2\tilde{v}_r(1) + \tilde{U}_1\tilde{v}_r(2)\right)\end{aligned} \tag{22}$$

If $F(1,2) \equiv \tilde{U}_1\tilde{U}_2$, then $\langle F\rangle = \langle\tilde{U}_1\tilde{U}_2\rangle$, where $\langle\,\cdot\,\rangle = \int \cdot\, \mathrm{d}y_+/L_y$, $y_+ = (y_1 + y_2)/2$ is a "zonal" average, and $F = \langle F\rangle + \tilde{F}$, $\tilde{F} = \widetilde{U_1U_2}$. $\langle\tilde{U}_1\tilde{U}_2\rangle$ is the mean PV correlation, and $\widetilde{U_1U_2}$ is fluctuation in correlation induced by advection. The asymmetric parts of $\tilde{U}_1\tilde{U}_2$ vanish after averaging in y_+, i.e. $\langle\widetilde{U_1U_2}\rangle = 0$, so we can separate (22) into the mean and fluctuating

parts like below,

$$\begin{aligned}
&\partial_t \left\langle \tilde{U}_1 \tilde{U}_2 \right\rangle + \partial_{r_1} \left\langle \tilde{v}_{r_1} \widetilde{U_1 U_2} \right\rangle + \partial_{y_1} \left\langle \tilde{v}_{y_1} \widetilde{U_1 U_2} \right\rangle + (1 \leftrightarrow 2) \\
&\quad = -\frac{3}{2} \Omega_D \left\langle \tilde{U}_2 \partial_{y1} \widetilde{T}_i(1) \right\rangle + C_i \partial_r (\overline{\Delta} \phi_Z) \left\langle \tilde{U}_2 \tilde{v}_r(1) \right\rangle \qquad (23) \\
&\qquad + (1 \leftrightarrow 2) \\
&\qquad\quad \partial_t \widetilde{U_1 U_2} + \partial_{r_1} \left(\tilde{v}_{r_1} \widetilde{U_1 U_2} \right) + \partial_{y_1} \left(\tilde{v}_{y_1} \widetilde{U_1 U_2} \right) \\
&\qquad\qquad + (1 \leftrightarrow 2) + \mathbf{V}_Z \left(\partial_{y_1} + \partial_{y_2} \right) \widetilde{U_1 U_2} \qquad (24) \\
&\qquad\qquad = -\tilde{\mathbf{v}}_1 \cdot \nabla \left\langle \tilde{U}_1 \tilde{U}_2 \right\rangle - \tilde{\mathbf{v}}_2 \cdot \nabla \left\langle \tilde{U}_1 \tilde{U}_2 \right\rangle
\end{aligned}$$

Nonlinear triplet terms in equation (23) require a closure. For a test mode in the form of $e^{i\mathbf{k}\cdot\mathbf{x}}$, $\widetilde{U_1 U_2}$ will respond at two different points, and thus drive a two-point response of the form $\tilde{F}_k \simeq \left[e^{i\mathbf{k}\cdot\mathbf{x}_1}() + e^{i\mathbf{k}\cdot\mathbf{x}_2}() \right]$. With such a response, we can close those terms like $\langle \tilde{v}_{r_1} \widetilde{U_1 U_2} \rangle$. Notice the homogeneity in y and inhomogeneity in r! Therefore a Fourier expansion in the y direction is applied.

$$\left\langle \tilde{v}_{r_1} \widetilde{U_1 U_2} \right\rangle = \left\langle \sum_{k_y} \underset{r}{\tilde{v}_{-k_y}} e^{-ik_y y_1} \left(\widetilde{U_1 U_2} \right)_{k_y} \right\rangle \qquad (25)$$

in which at a given position, for example (r_1, y_1), the velocity $\tilde{v}_r(r_1, y_1)$ and $\tilde{v}_y(r_1, y_1)$ can have the following Fourier transformation:

$$\tilde{v}_r(r_1, y_1) = \sum_{k_y} \underset{r}{\tilde{v}_{k_y}}(r_1) e^{ik_y y}, \quad \text{and} \quad \tilde{v}_y(r_1, y_1) = \sum_{k_y} \underset{y}{\tilde{v}_{k_y}}(r_1) e^{ik_y y} \qquad (26)$$

With this two-point response and equation (24), the quasi-linear expression is written as

$$\begin{aligned}
\left(\widetilde{U_1 U_2} \right)_{\substack{k_y \\ \omega}} = -\Bigg[& R^{(1)}_{\substack{k_y \\ \omega}} \underset{r}{\tilde{v}_{k_y}}(x_1) e^{ik_y y_1} \partial_{r_1} + R^{(1)}_{\substack{k_y \\ \omega}} \underset{y}{\tilde{v}_{k_y}}(x_1) e^{ik_y y_1} \partial_{y_1} \\
& + R^{(2)}_{\substack{k_y \\ \omega}} \underset{r}{\tilde{v}_{k_y}}(x_2) e^{ik_y y_2} \partial_{r_2} + R^{(2)}_{\substack{k_y \\ \omega}} \underset{y}{\tilde{v}_{k_y}}(x_2) e^{ik_y y_2} \partial_{y_2} \Bigg] \left\langle \tilde{U}_1 \tilde{U}_2 \right\rangle
\end{aligned}$$

where $R^{(1)}_{k_y,\omega} = i/(\omega - k_y V_Z + \frac{i}{\tau_c})$ is the response function for δf to $\tilde{\phi}$, the upper index (1) is an indication of location of velocities $\tilde{v}_r(r_1, y_1)$ and $\tilde{v}_y(r_1, y_1)$. The shear in zonal potential can shift the frequency, and hence change the correlation time. τ_c is the correlation time of $\tilde{U}$. Then all the nonlinear correlation terms, like $\langle \tilde{v}_{r_1} \widetilde{U_1 U_2} \rangle$, in the evolution of $\langle \tilde{U}_1 \tilde{U}_2 \rangle$, the

equation (23), can be calculated. In particular:

$$
\begin{aligned}
T_1 &= \partial_{r_1} \left\langle \tilde{v}_{r_1} \widetilde{U_1 U_2} \right\rangle \\
&= -\Bigg\langle \partial_{r_1} \sum_{k_y} \Bigg[R^{(1)}_{\substack{k_y \\ \omega}} \left| \tilde{v}_{\substack{k_y \\ r}}(x_1) \right|^2 \partial_{r_1} \\
&\qquad + R^{(2)}_{\substack{k_y \\ \omega}} \tilde{v}_{\substack{-k_y \\ r}}(x_1) \tilde{v}_{\substack{k_y \\ r}}(x_2) e^{ik_y(y_2-y_1)} \partial_{r_2} \\
&\qquad + R^{(1)}_{\substack{k_y \\ \omega}} \tilde{v}_{\substack{-k_y \\ r}}(x_1) \tilde{v}_{\substack{k_y \\ y}}(x_1) \partial_{y_1} \\
&\qquad + R^{(2)}_{\substack{k_y \\ \omega}} \tilde{v}_{\substack{-k_y \\ r}}(x_1) \tilde{v}_{\substack{k_y \\ y}}(x_2) e^{ik_y(y_2-y_1)} \partial_{y_2} \Bigg] \left\langle \tilde{U}_1 \tilde{U}_2 \right\rangle \Bigg\rangle \\
&\equiv -\partial_{r_1} \left(D^{r,r}_{1,1} \partial_{r_1} + D^{r,r}_{1,2} \partial_{r_2} + D^{r,y}_{1,1} \partial_{y_1} + D^{r,y}_{1,2} \partial_{y_2} \right) \left\langle \tilde{U}_1 \tilde{U}_2 \right\rangle
\end{aligned}
$$

and:

$$
\begin{aligned}
T_2 &= \partial_{r_2} \left\langle \tilde{v}_{r_2} \widetilde{U_1 U_2} \right\rangle \\
&= -\partial_{r_2} \left(D^{r,r}_{2,1} \partial_{r_1} + D^{r,r}_{2,2} \partial_{r_2} + D^{r,y}_{2,1} \partial_{y_1} + D^{r,y}_{2,2} \partial_{y_2} \right) \left\langle \tilde{U}_1 \tilde{U}_2 \right\rangle \\
T_3 &= \partial_{y_1} \left\langle \tilde{v}_{y_1} \widetilde{U_1 U_2} \right\rangle \\
&= -\partial_{y_1} \left(D^{y,r}_{1,1} \partial_{r_1} + D^{y,r}_{1,2} \partial_{r_2} + D^{y,y}_{1,1} \partial_{y_1} + D^{y,y}_{1,2} \partial_{y_2} \right) \left\langle \tilde{U}_1 \tilde{U}_2 \right\rangle \\
T_4 &= \partial_{y_2} \left\langle \tilde{v}_{y_2} \widetilde{U_1 U_2} \right\rangle \\
&= -\partial_{y_2} \left(D^{y,r}_{2,1} \partial_{r_1} + D^{y,r}_{2,2} \partial_{r_2} + D^{y,y}_{2,1} \partial_{y_1} + D^{y,y}_{2,2} \partial_{y_2} \right) \left\langle \tilde{U}_1 \tilde{U}_2 \right\rangle
\end{aligned}
$$

We can transform those terms involving only the derivatives in the y direction into relative coordinates, and use the symmetry of averaged quantities, i.e. $\partial_{y_+} \langle \tilde{U}_1 \tilde{U}_2 \rangle = 0$.

$$
\begin{aligned}
r_\pm &= \frac{r_1 \pm r_2}{2}, \qquad & \frac{\partial}{\partial r_{1,2}} &= \frac{1}{2} \left(\frac{\partial}{\partial r_+} \pm \frac{\partial}{\partial r_-} \right) \\
y_\pm &= \frac{y_1 \pm y_2}{2}, \qquad & \frac{\partial}{\partial y_{1,2}} &= \frac{1}{2} \left(\frac{\partial}{\partial y_+} \pm \frac{\partial}{\partial y_-} \right)
\end{aligned}
$$

For example,

$$
\begin{aligned}
&\partial_{y_1} \underset{1,1}{D^{y,y}} \partial_{y_1} + \partial_{y_1} \underset{1,2}{D^{y,y}} \partial_{y_2} + \partial_{y_2} \underset{2,1}{D^{y,y}} \partial_{y_1} + \partial_{y_2} \underset{2,2}{D^{y,y}} \partial_{y_2} \\
&= \frac{1}{4} \Bigg[\left(\partial_{y_+} - \partial_{y_-}\right) \underset{1,1}{D^{y,y}} \left(\partial_{y_+} - \partial_{y_-}\right) + \left(\partial_{y_+} - \partial_{y_-}\right) \underset{1,2}{D^{y,y}} \\
&\qquad \times \left(\partial_{y_+} + \partial_{y_-}\right) + \left(\partial_{y_+} + \partial_{y_-}\right) \underset{2,1}{D^{y,y}} \left(\partial_{y_+} - \partial_{y_-}\right) \\
&\qquad + \left(\partial_{y_+} + \partial_{y_-}\right) \underset{2,2}{D^{y,y}} \left(\partial_{y_+} + \partial_{y_-}\right) \Bigg] \\
&\approx \frac{1}{4} \partial_{y_-} \left(\underset{1,1}{D^{y,y}} + \underset{2,2}{D^{y,y}} - \underset{1,2}{D^{y,y}} - \underset{2,1}{D^{y,y}} \right) \partial_{y_-}
\end{aligned}
$$

Then we have $T_1 + T_2 + T_3 + T_4 = T_r + T_{y-} + T_{\text{cross}}$. Here T_r involves only derivatives in r, T_{y-} only contains derivatives in y_-, while T_{cross} has both. In the term T_{cross}, we can extract terms like $\underset{1,2}{D^{r,y}} - \underset{1,1}{D^{r,y}} + \underset{2,2}{D^{r,y}} - \underset{2,1}{D^{r,y}}$ or $\underset{1,1}{D^{y,r}} + \underset{1,2}{D^{y,r}} - \underset{2,2}{D^{y,r}} - \underset{2,1}{D^{y,r}}$, which will vanish for $1 \to 2$. Thus all cross terms vanish! The equation (23) for $\langle \tilde{U}_1 \tilde{U}_2 \rangle$ then is written below as:

$$
\begin{aligned}
&\partial_t \left\langle \tilde{U}_1 \tilde{U}_2 \right\rangle + T_r(1,2) + T_{y-}(1,2) \\
&\quad = -\frac{3}{2} \Omega_D \left(\left\langle \tilde{U}_2 \partial_{y1} \widetilde{T}_i(1) \right\rangle + \left\langle \tilde{U}_1 \partial_{y2} \widetilde{T}_i(2) \right\rangle \right) \\
&\qquad + C_i \partial_r (\overline{\Delta} \phi_Z) \left(\left\langle \tilde{U}_2 \tilde{v}_r(1) \right\rangle + \left\langle \tilde{U}_1 \tilde{v}_r(2) \right\rangle \right)
\end{aligned} \tag{27}
$$

with,

$$
\begin{aligned}
T_r(1,2) &= -\Bigg(\partial_{r1} \underset{1,1}{D^{r,r}} \partial_{r1} + \partial_{r2} \underset{2,2}{D^{r,r}} \partial_{r2} \\
&\qquad + \partial_{r1} \underset{1,2}{D^{r,r}} \partial_{r2} + \partial_{r2} \underset{2,1}{D^{r,r}} \partial_{r1} \Bigg) \left\langle \tilde{U}_1 \tilde{U}_2 \right\rangle \\
T_{y-}(1,2) &= -\frac{1}{4} \partial_{y_-} \Bigg(\underset{1,1}{D^{y,y}} + \underset{2,2}{D^{y,y}} \\
&\qquad - \underset{1,2}{D^{y,y}} - \underset{2,1}{D^{y,y}} \Bigg) \partial_{y_-} \left\langle \tilde{U}_1 \tilde{U}_2 \right\rangle
\end{aligned}
$$

Equation (27) is the 2-point correlation evolution equation (for $\langle \tilde{U}_1 \tilde{U}_2 \rangle$) we need. As mentioned in the road map, we will use it to get the evolution equation for $\langle \tilde{\phi}^2 \rangle$.

Some simplifications of T_r and T_{y-} will be useful in the next subsection. In $T_r(1,2)$, derivatives with respect to r_- probe the dependence of correlation on separation in r, which will vanish as $r_- \to 0$. *Derivatives relevant to r_+ are sensitive to mean profile.* Extracting all terms only involving ∂_{r_+} obtains $T_r(1,2) = -\partial_{r_+} D_{r,r} \partial_{r_+} \langle \tilde{U}_1 \tilde{U}_2 \rangle + \cdots$. For $D_{r,r}$ in T_r,

when we take the limit of $r_- \to 0$, there is:

$$\begin{aligned} D_{r,r} &= \lim_{r_1 \to r_2} \left(\underset{1,1}{D^{r,r}} + \underset{1,2}{D^{r,r}} + \underset{2,1}{D^{r,r}} + \underset{2,2}{D^{r,r}} \right) \\ &= \lim_{r_1 \to r_2} \sum_{k_y} \left[\underset{\omega}{R^{(1)}_{k_y}} \left| \underset{r}{\tilde{v}_{k_y}}(r_1) \right|^2 + \underset{\omega}{R^{(2)}_{k_y}} \left| \underset{r}{\tilde{v}_{k_y}}(r_2) \right|^2 \right. \\ &\quad + \underset{\omega}{R^{(2)}_{k_y}} \underset{r}{\tilde{v}_{-k_y}}(r_1) \underset{r}{\tilde{v}_{k_y}}(r_2) e^{ik_y(y_2 - y_1)} \\ &\quad \left. + \underset{\omega}{R^{(1)}_{k_y}} \underset{r}{\tilde{v}_{-k_y}}(r_2) \underset{r}{\tilde{v}_{k_y}}(r_1) e^{ik_y(y_1 - y_2)} \right] \\ &= 2 \sum_{k_y} \underset{\omega}{R_{k_y}} k_y^2 \left| \tilde{\phi}_k \right|^2 (1 + \cos(k_y y_-)) \end{aligned} \tag{28}$$

There is a summation in k_y determined by the distribution of $\langle \tilde{\phi}_k^2 \rangle$ in k_y. In the following discussion, the approximate values of $D_{r,r}$ are determined by the expansion of $\langle \tilde{\phi}^2 \rangle$ in the y_- direction. To characterize the expansion, we can define the second moment of y_- by:

$$\left\langle y_-^2 \right\rangle = \frac{\int y_-^2 \left\langle \tilde{\phi}^2 \right\rangle (r, y_-) \mathrm{d}y_-}{\int \left\langle \tilde{\phi}^2 \right\rangle (r, y_-) \mathrm{d}y_-}$$

We consider the two cases for $\langle y_-^2 \rangle$:

- When most $\langle \tilde{\phi}_k^2 \rangle (r, y_-)$ is expanded in y_- (i.e. $\langle y_-^2 \rangle \to 0$), contributions to the summation in equation (28) will be concentrated where $k_y y_- \sim 0$, therefore leading to the approximation $\cos(k_y y_-) \approx 1$.
- When we examine $\langle \tilde{\phi}_k^2 \rangle (r, y_-)$ for large y_- (i.e. $\langle y_-^2 \rangle > 1$), the summation concentrates on those $\langle \tilde{\phi}_k^2 \rangle$ with $k_y y_- > 1$ and $\cos(k_y y_-)$ oscillates rapidly. Therefore the summation in equation (28) of $\cos(k_y y_-)$ decays.

To conclude this discussion, equation (28) leads to:

$$D_{r,r} \approx \begin{cases} 4D_0 \left\langle \tilde{\phi}^2 \right\rangle, \text{when } \left\langle y_-^2 \right\rangle \to 0, \\ 2D_0 \left\langle \tilde{\phi}^2 \right\rangle, \text{when } \left\langle y_-^2 \right\rangle > 1. \end{cases}$$

Here $D_0 = \sum_{k_y} \underset{\omega}{R_{k_y}} k_y^2 \left| \tilde{\phi}_k \right|^2 / \langle \tilde{\phi}^2 \rangle$.

Similarly for T_{y_-} and $D_{y,y}$, we let $r_- \to 0$, but keep the y_- dependence,

$$\begin{aligned} D_{y,y} &= \lim_{r_1 \to r_2} \left(\underset{1,1}{D^{y,y}} + \underset{2,2}{D^{y,y}} - \underset{1,2}{D^{y,y}} - \underset{2,1}{D^{y,y}} \right) \\ &\approx 2 \sum_{k_y} \underset{\omega}{R_{k_y}} \left| \tilde{\phi}_k \right|^2 \frac{k_y^2}{k_y^2 l_r^2} (1 - \cos(k_y y_-)) \end{aligned}$$

Here l_r is the correlation length of modes, which is approximately several ρ_i. When $\langle y_-^2 \rangle \to 0$, we have $1 - \cos(k_y y_-) \simeq (k_y y_-)^2/2$, which results in $\langle y_-^2 \rangle$ after summation. On the other hand, when $\langle y_-^2 \rangle > 1$, summation over $\cos k_y y_-$ vanishes. The results are:

$$D_{y,y} = \begin{cases} D_0 \left\langle \tilde{\phi}^2 \right\rangle \dfrac{\langle y_-^2 \rangle}{l_r^2}, \text{when } \langle y_-^2 \rangle \to 0, \\ 2D_0 \left\langle \tilde{\phi}^2 \right\rangle \dfrac{1}{\overline{k}_y^2 l_r^2}, \text{when } \langle y_-^2 \rangle > 1. \end{cases}$$

We notice that both $D_{r,r}$ and $D_{y,y}$ are determined by the scale of $\langle y_-^2 \rangle$. If we start from the case of the small argument expansion of $\langle \tilde{\phi}_k^2 \rangle$ in y_-, which corresponds to $\langle y_- \rangle = 0$ and $\langle y_-^2 \rangle \to 0$, then the evolution equation gives:

$$\frac{\partial}{\partial t} \langle y_-^2 \rangle = \frac{\int y_-^2 \dfrac{\partial}{\partial y_-} D_{y,y} \dfrac{\partial}{\partial y_-} \left\langle \tilde{\phi}^2 \right\rangle \mathrm{d}y_-}{\int \left\langle \tilde{\phi}^2 \right\rangle (r, y_-) \mathrm{d}y_-}$$

$$\sim 2 \frac{\int D_{y,y} \left\langle \tilde{\phi}^2 \right\rangle \mathrm{d}y_-}{\int \left\langle \tilde{\phi}^2 \right\rangle (r, y_-) \mathrm{d}y_-} \propto 2D_0 \left\langle \tilde{\phi}^2 \right\rangle \frac{\langle y_-^2 \rangle}{l_r^2}$$

Integrating in time yields,

$$\langle y_-^2 \rangle \propto \exp\left(2D_0 \left\langle \tilde{\phi}^2 \right\rangle \frac{t}{l_r^2} \right)$$

This means when $\langle y_-^2 \rangle$ is small, $\langle y_-^2 \rangle$ will grow in y_- exponentially in time, until y_- reaches the scale of several $1/\overline{k}_y$. Then both $D_{r,r}$ and $D_{y,y}$ enter the case where $\langle y_-^2 \rangle$ is large. So we will focus on the limit of large $\langle y_-^2 \rangle$ in the rest of this paper:

$$D_{r,r} = 2D_0 \left\langle \tilde{\phi}^2 \right\rangle \tag{29}$$

$$D_{y,y} = 2D_0 \left\langle \tilde{\phi}^2 \right\rangle \frac{1}{\overline{k}_y^2 l_r^2} \tag{30}$$

Following the road map at the beginning of this section, we will apply the double Green's function to (27) to obtain the evolution equation of correlation function $\langle \tilde{\phi}_1 \tilde{\phi}_2 \rangle$, just as the definition in equation (20).

B. From Potential Enstrophy to Potential Intensity Evolution

Based on equation (27), we apply the double Green's function for $\tilde{U}$, then take the limit $r_1 \to r_2$, and thus obtain the $\langle \tilde{\phi}^2 \rangle$ evolution equation. The Green's function used in (20)

and (27) is based on the inverse Fourier transform of (19):

$$\mathcal{G}(x) = \frac{1}{\delta_b^2}\mathscr{F}^{-1}\left\{\frac{1}{A+k^2}\right\} = \frac{\sqrt{A}}{2}e^{-\sqrt{A}|x|}$$
$$\mathcal{G}(x,x') = \frac{\sqrt{A}}{2}e^{-\sqrt{A}|x-x'|} \tag{31}$$

where $A = C_e/(C_i\delta_b^2) = \tau/(\sqrt{2\varepsilon_0}\delta_b^2) \sim \delta_b^{-2}$. δ_b is the banana width, which averages over structure on scales less than δ_b. Thus any structure convolved with this Green's function must be of order of δ_b or coarser. The full inverse Fourier transformation of $1/(1+\delta_b^2k_r^2+\rho_i^2k_y^2)$ leads to a modified Bessel function of the second kind $K_0(\sqrt{(r/\delta_b)^2+(y/\rho_i)^2})$. We neglected the k_y dependence in the equation above since $k_y\rho_i \ll k_r\delta_b$. We first deal with the R.H.S of the equation (27). Terms related to zonal flow may restrict turbulence propagation, and the zonal flow effects on turbulence spreading is still under study [10, 26, 27]. For simplicity, hereafter, we neglect the coupling to zonal potential. As for the term containing the fluctuating temperature and curvature drift, there is:

$$\begin{aligned}
&\frac{A}{4}\iint e^{-\sqrt{A}(|r_1'-r_1|+|r_2'-r_2|)}\Big(\left\langle\tilde{U}_{2'}\partial_{y_{1'}}\tilde{T}_{1'}\right\rangle \\
&\quad+\left\langle\tilde{U}_{1'}\partial_{y_{2'}}\tilde{T}_{2'}\right\rangle\Big)\mathrm{d}r_1'\mathrm{d}r_2' \\
&=\frac{\sqrt{A}}{2}\Big(\int e^{-\sqrt{A}|r_1'-r_1|}\left\langle\tilde{\phi}_2\partial_{y_{1'}}\tilde{T}_{1'}\right\rangle\mathrm{d}r_1' \\
&\quad+\int e^{-\sqrt{A}|r_2'-r_2|}\left\langle\tilde{\phi}_1\partial_{y_{2'}}\tilde{T}_{2'}\right\rangle\mathrm{d}r_2'\Big)
\end{aligned}$$

The Green's function will transform $\tilde{U}$ into $\tilde{\phi}$. Taking limit of $r_1 \to r_2$ yields the equation as below. Since the average bracket is over y_+, we can integrate the result by parts, yielding:

$$\begin{aligned}
&2\frac{\sqrt{A}}{2}\int e^{-\sqrt{A}|r'-r|}\left\langle\tilde{\phi}\partial_y\tilde{T}\right\rangle\mathrm{d}r \\
&=\sqrt{A}\int e^{-\sqrt{A}|r'-r|}\left\langle\tilde{v}_r\tilde{T}\right\rangle\mathrm{d}r'
\end{aligned} \tag{32}$$

This represents a distributed pumping of $\langle\tilde{\phi}^2\rangle$ from the heat flux $\langle\tilde{v}_r\tilde{T}\rangle$. We call it the nonlocal growth term. The nonlocal convolution kernel has a width of several δ_b, thus the growth of $\langle\tilde{\phi}^2\rangle$ at r is affected by a region of several δ_b in width.

Since $\delta_b/L_T \ll 1$, thus what we obtain is a *modest* nonlocal effect. There are two preconditions for such nonlocal growth to exist:

- First is the curvature of the field, which causes trapped ion orbit and ion-precessional motion.

- Second is the polarization charge due to trapped ions, resulting in redistribution of fluctuating temperature.

On the time scale $\tau > \tau_b$, these processes cause nonlocal growth effects, where τ_b is the trapped particle bounce time. To clarify, such nonlocal pump can exist where linear instability of trapped ion mode is absent. Because the linear response sets eigenmode or spatial form factor dependence, but the growth of $\langle\tilde{\phi}^2\rangle$ is not a result only of linear amplification.

For T_r in the L.H.S of equation (27), applying the double Green's function results in

$$\iint \mathcal{G}(x_1, x_1')\mathcal{G}(x_2, x_2')T_r(1', 2')\mathrm{d}x_1'\mathrm{d}x_2'$$

Since $l_s > \delta_b$ (i.e. length scale of correlation function exceeds the banana width), we can expand $T_r(1', 2')$ around points x_1 and x_2 as:

$$\begin{aligned}
T_r(1', 2') &= T_r(1, 2) \\
&+ \left[(r_1' - r_1)\frac{\partial}{\partial r_1} + (r_2' - r_2)\frac{\partial}{\partial r_2}\right] T_r(1, 2) \\
&+ \frac{1}{2}\Bigg[(r_1' - r_1)^2\frac{\partial^2}{\partial r_1^2} + (r_2' - r_2)^2\frac{\partial^2}{\partial r_2^2} \\
&\qquad + 2(r_1' - r_1)(r_2' - r_2)\frac{\partial}{\partial r_1}\frac{\partial}{\partial r_2}\Bigg] T_r(1, 2) + \cdots \\
&= \sum_{m=0,n=0}^{\infty} \frac{T_r^{(m,n)}}{\Gamma(m+1)\Gamma(n+1)}(r_1 - r_1')^m(r_2 - r_2')^n
\end{aligned}$$

Here $\Gamma(m+1) = m!$, for m an integer, is the Gamma function, and

$$\begin{aligned}
T_r^{(m,n)} &\equiv C_{m+n}^m \partial_{r_1}^m \partial_{r_2}^n T_r(1, 2) \\
&= \frac{C_{m+n}^m}{2^{m+n}} \partial_{r_+}^{m+n} T_r(1, 2) + \cdots
\end{aligned}$$

Some useful relations for C_{m+n}^m are used in following derivation. These are:

$$\sum_{m=0}^{m+n} C_{m+n}^m = 2^{m+n}, \tag{33}$$

$$\sum_{\substack{m=0, \\ \text{mod } (m,2)=0}}^{m+n} C_{m+n}^m = 2^{m+n-1}, m+n \neq 0 \tag{34}$$

When the Green's function convolutions are applied to $T_r(1,2)$, only those terms with both m and n even will survive in the integral, because the convolution kernel itself is an even function in r. Thus,

$$\begin{aligned}
&\frac{A}{4}\iint e^{-\sqrt{A}|r_1'-r_1|-\sqrt{A}|r_2'-r_2|}T_r(1',2')\mathrm{d}r_1'\mathrm{d}r_2' \\
&\quad=\frac{A}{4}\sum_{m=0,n=0}^{\infty}\frac{T_r^{(m,n)}}{\Gamma(m+1)\Gamma(n+1)} \\
&\times\iint e^{-\sqrt{A}(|r_1'-r_1|+|r_2'-r_2|)}(r_1-r_1')^m(r_2-r_2')^n\mathrm{d}r_1'\mathrm{d}r_2' \\
&\quad=\frac{A}{4}\sum_{\substack{m=0,n=0\\ \bmod(m,2)=0\\ \bmod n,2=0}}^{\infty}\frac{C_{m+n}^m}{2^{m+n}}\partial_{r_+}^{m+n}T_r(1,2)\frac{2}{A^{\frac{m+1}{2}}}\frac{2}{A^{\frac{n+1}{2}}}
\end{aligned}\tag{35}$$

where the integrations are cancelled by the Gamma functions. Rewriting $k\equiv m+n$ and using equation (34), the equation above is rewritten as:

$$\begin{aligned}
&\frac{1}{2}T_r(1,2)+\frac{1}{2}\sum_{\substack{k=0\\ \bmod(k,2)=0}}^{\infty}\frac{1}{A^{\frac{k}{2}}}\partial_{r_+}^k T_r(1,2) \\
&=\frac{1}{2}T_r(1,2)+\frac{\sqrt{A}}{4}\int e^{-\sqrt{A}|r_+'-r_+|}T_r(1',2')\mathrm{d}r_+'
\end{aligned}$$

or equivalently,

$$\left(\frac{1}{2}+\frac{1}{2}\mathcal{G}(r_+)\otimes\right)T_r(1,2)\tag{36}$$

Here we define $\mathcal{G}(r_+)=\frac{\sqrt{A}}{2}e^{-\sqrt{A}|r_+|}$, and $f(x)\otimes g(x)=\int f(x-x')g(x')\mathrm{d}x'$ is a convolution. The dependence on r_+ in $T_r(1,2)$ is implicit. After taking limit of $r_1\to r_2$, $T_r(1,2)$ will lead to diffusion. Since this formula involves the same convolution as in equation (32), and since the expression above will introduce effects from other locations, we call (36) the *nonlocal diffusion* term, for consistency. We emphasis that this is a *modest* nonlocal effect.

Actually, the polarization terms $\overline{\Delta}\tilde{\phi}$ in the kinetic equation are approximations to the lowest order, with $\delta_b\ll 1$[18]. When δ_b is not so small, the convolution kernel can be asymmetric, thus the integrals for even m or n could be non-zero. Based on this, we argue that for the integral to not vanish, the constraints of m and n even could be loosened to $m+n$ even.

As a result, we use the expression below, instead of equation (36), to investigate the effect

of nonlocal diffusion.

$$\begin{aligned}\frac{A}{4}\iint e^{-\sqrt{A}|r_1'-r_1|-\sqrt{A}|r_2'-r_2|}T_r(1',2')\mathrm{d}r_1'\mathrm{d}r_2' \\ \sim \frac{\sqrt{A}}{2}\int e^{-\sqrt{A}|r_+'-r_+|}T_r(1',2')\mathrm{d}r_+' \\ = \mathcal{G}(r_+)\otimes T_r(1,2)\end{aligned} \tag{37}$$

All terms including derivatives with respect to r_- are neglected here and below.

The next step is taking the limit of $r_1 \to r_2$ in equation (37). Using the definition of $\tilde{U}$, we obtain,

$$\begin{aligned}\left\langle \tilde{U}(1)\tilde{U}(2)\right\rangle &\sim \left\langle \left(\tilde{\phi}(1)-\delta_b^2\partial_{r1}^2\tilde{\phi}(1)\right)\left(\tilde{\phi}(2)-\delta_b^2\partial_{r2}^2\tilde{\phi}(2)\right)\right\rangle \\ &= \left\langle \tilde{\phi}(1)\tilde{\phi}(2)\right\rangle - \delta_b^2\left(\partial_{r_1}^2+\partial_{r_2}^2\right)\left\langle \tilde{\phi}(1)\tilde{\phi}(2)\right\rangle + \cdots\end{aligned}$$

In the limit $r_1 \to r_2$, with equation above, we have T_r:

$$\begin{aligned}&\lim_{r_1\to r_2} T_r(1,2) \\ &= -\lim_{r_1\to r_2}\left[\frac{1}{4}\partial_{r_+}\left(D_{1,1}^{r,r}+D_{2,2}^{r,r}+D_{1,2}^{r,r}+D_{2,1}^{r,r}\right)\partial_{r_+}+\cdots\right] \\ &\quad\times\left[\left\langle\tilde{\phi}(1)\tilde{\phi}(2)\right\rangle-\frac{\delta_b^2}{2}\partial_{r_+}^2\left\langle\tilde{\phi}(1)\tilde{\phi}(2)\right\rangle+\cdots\right] \\ &= -\partial_{r_+}D_{r_+,r_+}\partial_{r_+}\left[\left\langle\tilde{\phi}^2\right\rangle-\frac{\delta_b^2}{2}\partial_{r_+}^2\left\langle\tilde{\phi}^2\right\rangle\right]\end{aligned} \tag{38}$$

Substituting T_r above into (37), together with the heat flux drive (32), we obtain the ultimate evolution equation of $\langle\tilde{\phi}^2\rangle$, where we replaced r_+ by r. That is:

$$\begin{aligned}\partial_t\left\langle\tilde{\phi}^2\right\rangle = &\frac{\sqrt{A}}{2}\int e^{-\sqrt{A}|r'-r|} \\ &\times\frac{\partial}{\partial r'}\left[2D_0\left\langle\tilde{\phi}^2\right\rangle\frac{\partial}{\partial r'}\left(\left\langle\tilde{\phi}^2\right\rangle-\frac{\delta_b^2}{2}\frac{\partial^2}{\partial r'^2}\left\langle\tilde{\phi}^2\right\rangle\right)\right]\mathrm{d}r' \\ &-3\Omega_D\frac{\sqrt{A}}{2}\int e^{-\sqrt{A}|r'-r|}\left\langle\tilde{v}_r\tilde{T}\right\rangle(r')\mathrm{d}r' \\ &+\frac{1}{2}\partial_{y_-}D_{y,y}\partial_{y_-}\left\langle\tilde{\phi}^2\right\rangle\end{aligned} \tag{39}$$

If we neglect all nonlocal effects and δ_b-related terms in this equation, we obtain:

$$\begin{aligned}\partial_t\left\langle\tilde{\phi}^2\right\rangle = &\frac{\partial}{\partial r}D_{r,r}\frac{\partial}{\partial r}\left\langle\tilde{\phi}^2\right\rangle+\frac{1}{2}\partial_{y_-}D_{y,y}\partial_{y_-}\left\langle\tilde{\phi}^2\right\rangle \\ &-3\Omega_D\left\langle\tilde{v}_r\tilde{T}\right\rangle\end{aligned} \tag{40}$$

Recall the usual toy spreading model for weak turbulence [9–11]:

$$\partial_t \mathcal{E} = \partial_x[(D_0\mathcal{E})\partial_x\mathcal{E}] - \gamma_{\rm NL}\mathcal{E}^2 + \gamma\mathcal{E} = 0 \tag{41}$$

where $\mathcal{E}$ is the turbulence enstrophy [25]. We can see the similarity between equations (40) and (41). In particular, for the flux term in equation (40) (the first term on the R.H.S.), if we take the approximation $D_{r,r} = 2D_0\langle\tilde{\phi}^2\rangle$, as shown in the previous section (equation (29)), there is

$$\Gamma(\left\langle\tilde{\phi}^2\right\rangle) \sim 2D_0\langle\tilde{\phi}^2\rangle\partial_r\langle\tilde{\phi}^2\rangle$$

which recovers the intensity flux in the toy model. Furthermore, for $D_{y,y} = 2D_0\langle\tilde{\phi}^2\rangle/(\bar{k}_y^2 l_r^2)$ as shown in previous section equation (30) (N.B.: let's say $\partial_{y_-} \sim i\bar{k}_y$), then,

$$\partial_{y_-} D_{y,y}\partial_{y_-}\left\langle\tilde{\phi}^2\right\rangle \propto -\frac{2D_0}{l_r^2}\left\langle\tilde{\phi}^2\right\rangle^2$$

which gives the local dissipation, even when $r_- \to 0$. *This corresponds to the local nonlinear dissipation $-\gamma_{NL}\mathcal{E}^2$ in the toy model.* Using linear growth to replace the heat flux drive, we have:

$$\langle\tilde{v}_r\tilde{T}\rangle \sim -\left\langle\tilde{\phi}^2\right\rangle\partial_r\langle T\rangle \sim -\gamma_L\left\langle\tilde{\phi}^2\right\rangle$$

Here we already assumed $\partial_r\langle T\rangle \sim \langle T\rangle/L_T > 0$, and $\gamma \propto \langle T\rangle/L_T$. Finally, with all the above statements, we obtain,

$$\partial_t\left\langle\tilde{\phi}^2\right\rangle = \frac{\partial}{\partial r}\left(2D_0\left\langle\tilde{\phi}^2\right\rangle\frac{\partial}{\partial r}\left\langle\tilde{\phi}^2\right\rangle\right) + \gamma_L\left\langle\tilde{\phi}^2\right\rangle - \frac{D_0}{l_r^2}\left\langle\tilde{\phi}^2\right\rangle^2 \tag{42}$$

Equation (42) contains the essential nonlinear diffusion with local growth and damping, and has the same form as equation (41), as used before in Ref. [10, 11] for turbulence spreading. Observe there are some differences between our model and the conventional one. The most obvious difference is that our model concerns the evolution of $\langle\tilde{\phi}^2\rangle$, while the toy model describes the evolution of turbulence energy $\mathcal{E}$. And, importantly, we obtain the damping term by retaining the diffusion in y_- and the growth term from the curvature drift. These give more a detailed understanding of the physics than does the toy model.

Equation (42) is obtained for the condition $\delta_b \ll 1$. When we reinstate those nonlocal terms dropped before, we find:

$$\begin{aligned}\partial_t\left\langle\tilde{\phi}^2\right\rangle = \mathcal{G}\otimes\frac{\partial}{\partial r}\left[2D_0\left\langle\tilde{\phi}^2\right\rangle\frac{\partial}{\partial r}\left(\left\langle\tilde{\phi}^2\right\rangle - \frac{\delta_b^2}{2}\frac{\partial^2}{\partial r^2}\left\langle\tilde{\phi}^2\right\rangle\right)\right] \\ + \mathcal{G}\otimes\left(\gamma_L(r)\left\langle\tilde{\phi}^2\right\rangle\right) - \frac{D_0}{l_r^2}\left\langle\tilde{\phi}^2\right\rangle^2\end{aligned} \tag{43}$$

where equation (43) has both *nonlocal diffusion* (the first term on the R.H.S.), and *nonlocal growth* (the second term on the R.H.S.). We describe them as nonlocal effects since they involve convolutions and introduce dependence upon $r' \neq r$. These explicit nonlocal effects are modest, but can lead to a significant difference in turbulence spreading. These nonlocal terms highlight another difference between our results and the conventional model (41). A comparison between our model, the conventional model, and Dupree's two-point theory is displayed in Table I.

We can dedimensionalize equation (42) with:

$$t \to \frac{\hat{t}}{\gamma_L}, \qquad r \to \hat{r} L_T, \qquad \left\langle \tilde{\phi}^2 \right\rangle \to \hat{I} \frac{\gamma_L}{\gamma_{NL}}$$

where we used a constant linear growth γ_L and γ_L/γ_{NL} is the saturation level of $\langle \tilde{\phi} \rangle$. Then we have:

$$\frac{\partial}{\partial \hat{t}} \hat{I} = \frac{\partial}{\partial \hat{r}} \left(2 \hat{D}_0 \hat{I} \frac{\partial}{\partial \hat{r}} \hat{I} \right) + \hat{I} - \hat{I}^2 \tag{44}$$

Here,

$$\hat{D}_0 = \frac{D_0}{L_T^2 \gamma_{NL}} = \frac{D_0 l_r^2}{L_T^2 D_0} = \frac{l_r^2}{L_T^2}$$

The scale of l_r is roughly around ρ_i and limited by δ_b. In equation (30), because of the absent of detailed calculation of the spectrum (very challenging!), we set it to be around gyro-radius, i.e. $l_r \sim \rho_i$. This means the transport coefficient follows gyro-Bohm scaling $\hat{D}_0 \simeq (\rho/L_T)^2$. And therefore the model can also be compared to previous gyro-kinetic simulation results [28, 29]. There is only one parameter, the mode correlation length $l_{r*} \equiv l_r/L_T$, which is proportional to $\rho_* \equiv \rho_i/L_T$. For the corrected model equation (43), after dedimensionalizing we obtain,

$$\frac{\partial}{\partial \hat{t}} \hat{I} = \mathcal{G} \otimes \frac{\partial}{\partial \hat{r}} \left[2 \hat{D}_0 \hat{I} \frac{\partial}{\partial \hat{r}} \left(\hat{I} - \frac{\delta_{b*}^2}{2} \frac{\partial^2}{\partial \hat{r}^2} \hat{I} \right) \right] + \mathcal{G} \otimes \hat{I} - \hat{I}^2 \tag{45}$$

where δ_{b*} is dedimensionalized to L_T.

Because (45) is complicated, we try to simplify it by two different approaches, either keeping only nonlocal diffusion, like (46a), or only nonlocal growth, like (46b). Of course, the full simplification leads to equation (44).

$$\frac{\partial}{\partial \hat{t}} \hat{I} = \mathcal{G} \otimes \frac{\partial}{\partial \hat{r}} \left[2 \hat{D}_0 \hat{I} \frac{\partial}{\partial \hat{r}} \left(\hat{I} - \frac{\delta_{b*}^2}{2} \frac{\partial^2}{\partial \hat{r}^2} \hat{I} \right) \right] + \hat{I} - \hat{I}^2 \tag{46a}$$

$$\frac{\partial}{\partial \hat{t}} \hat{I} = \frac{\partial}{\partial \hat{r}} \left(2 \hat{D}_0 \hat{I} \frac{\partial}{\partial \hat{r}} \hat{I} \right) + \mathcal{G} \otimes \hat{I} - \hat{I}^2 \tag{46b}$$

TABLE I. Comparison between contentional model, our model and the Dupree's two-point theory

	Conventional models	Yan & Diamond	Dupree
Quantity I	$\langle\tilde{\phi}^2\rangle$ in Ref. [10].	$\langle\tilde{\phi}^2\rangle$	$\langle\tilde{f}_1\tilde{f}_2\rangle$
	Turbulence energy $\mathcal{E}$ in Ref.[11]		
	N_k and K_k in Ref.[26]		
Spatial dependence	r	r_+, y_-	r_-
$D(I)$	$\simeq D_0\varepsilon^\alpha$	$D_0\langle\tilde{\phi}^2\rangle$	$D_{\rm rel}$
γ_L	Local	Nonlocal	-
$\gamma_{\rm NL}$	Coupling to small structure	Expansion in y_-, D_0/l_r^2	-
Δ_p depends on	$\sim\sqrt{2D_0/\gamma_{\rm NL}}$	l_r, δ_b	-
Derivation methods	Phenomenology in Ref. [10]	2-p correlation,	2-p correlation
	Fokker-Planck and QL in Ref. [11]	Green's function	

We see there is another control parameter, the banana width δ_{b*}. Effectively, we can rescale the coordinate r to $r = \hat{\hat{r}}\delta_b/L_T^2$, and see the only parameter left in equation (45) is $\hat{\hat{D}}_0 = D_0 l_r^2/\delta_b^2$. Thus l_{r*} and the ratio of δ_{b*}/l_{r*} are the real control parameters. Changing the device size or L_T with fixed δ_{b*} and l_{r*} is effectively a rescaling of the coordinates.

We shall compare the difference between (44) and (45) to see the effects on turbulence spreading. More specifically, we aim to answer:

1. How do those nonlocal terms affect spreading front generation and propagation?

2. And more important, how do these terms affect the turbulence penetration depth into the linearly stable region? We expect that both nonlocal effects will broaden the propagating front, speed up the propagation and extend the penetration depth.

3. A key question is: which is more effective? Nonlocal diffusion or nonlocal growth? Therefore the two simplified equations (46a) and (46b) are compared with the original equation (45) to study which effect dominates.

4. Then how do these nonlocal effects affect the transport?

It's worthwhile to mention that, if we don't use the convolution, but simply add more high-order correction terms in equation (45), the numerical solution will generate negative values and fluctuate at the leading edge, see more details in the Appendix A. By calculating the convolution, we obtain better results.

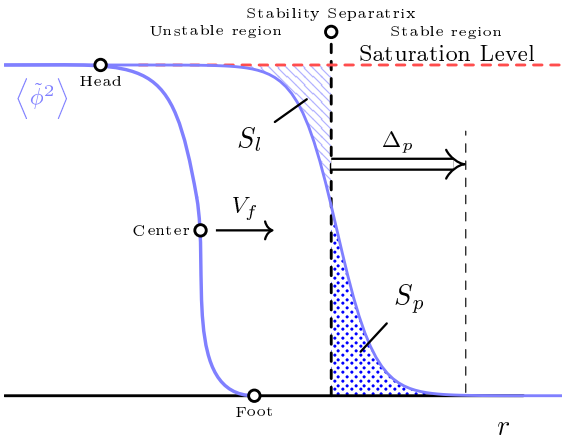

FIG. 2. Illustration of turbulence spreading: Definition of "Head", "Center" and "Foot" of the leading edge. Penetration depth Δ_p and effective penetration depth S_p are defined to characterize the spreading into stable region. S_l is the intensity lose from the unstable region.

IV. SOLVING THE INTENSITY EQUATION

In previous section, we derived the usual spreading model equation (44), and the corrected model equation (45-46b) (with nonlocal effects), from the kinetic equation.

Equation (44) has been studied intensively[10, 11, 26]. Based on these studies, we know the basic picture of spreading, as shown in figure 2. Turbulence grows in an unstable region and saturates at a certain level. A front of turbulence intensity (the leading edge) moving at a speed V_f is generated. We can define the "Head" and "Foot" of the leading edge by specifying where the profile reaches certain levels. Also, we define the point of maximum gradient as the "Center" of the leading edge. After the front reaches the border of the

unstable region, it will penetrate a distance into the stable region. To analyze how much turbulence penetrates into the stable region, we define several quantities. Δ_p is the position of the foot of the penetration front, and is given in units of L_T. S_p is the total area covered by the profile in the stable region, as shown in figure 2.

In order to answer the questions raised in the previous section, we study the turbulence spreading in models (45-46b) numerically. We use the 6th order finite difference method (FDM) in space and the usual 4th order Runge-Kutta method in time to investigate the evolution. The grid size is 10^{-3}, the time step is 10^{-3} (can be finer in some cases). One parameter in equation (44) is the l_r, scale or correlation length of modes. The another parameter in equations (45-46b) is the banana orbit width δ_{b*}. As we stated early, we let $l_r \sim \rho_i$, and we define

$$\rho_* \equiv \frac{\rho_i}{L_T} \sim 10^{-3} \text{ to } 10^{-2} \tag{47}$$

And there is [30],

$$\delta_{b*} \equiv \frac{\delta_b}{L_T} \sim \sqrt{\frac{R}{r}} q\rho_* \sim 10 \text{ to } 20\rho_* \tag{48}$$

where q is the safety factor.

Neumann boundaries are set by introducing ghost points $u_{-4}, \cdots, u_{-1}$ and $u_{N+1}, \cdots, u_{N+4}$ outside the boundary, and let,

$$\begin{aligned} u_{-4} = u_4, \cdots, u_{-1} = u_1 \\ u_{N+1} = u_N, \cdots, u_{N+4} = u_{N-3} \end{aligned} \tag{49}$$

Such a boundary condition works fine except for equation (45) and (46b), which involve the nonlocal growth term. Because the FDM used here is of 6th order, there are at least 3 points required on both sides of a boundary point. In practice, we find that to make boundaries stable, there are at least 4 ghost points needed. Therefore, the boundary point is implicitly at the middle of u_{-1} and u_1 or u_N and u_{N+1}. But as long as the boundaries are set far enough away from the evolving leading edge, they will not affect our conclusions.

To get an intuitive impression of the difference between equation (44) and equation (45), we set the unstable regions as in figure 3(a) as an example. And we also set $l_{r*} = \rho_* = 0.01$ and $\delta_{b*} = 0.1$. There are two separate unstable regions. Turbulence grows in the left unstable region, then penetrates into the stable region, and can even spread into the right unstable region. The intensity saturates at 1, which is the "gyro-Bohm" level. For equation (44), the leading edges of the intensity profile have almost no discernable distance between "Center"

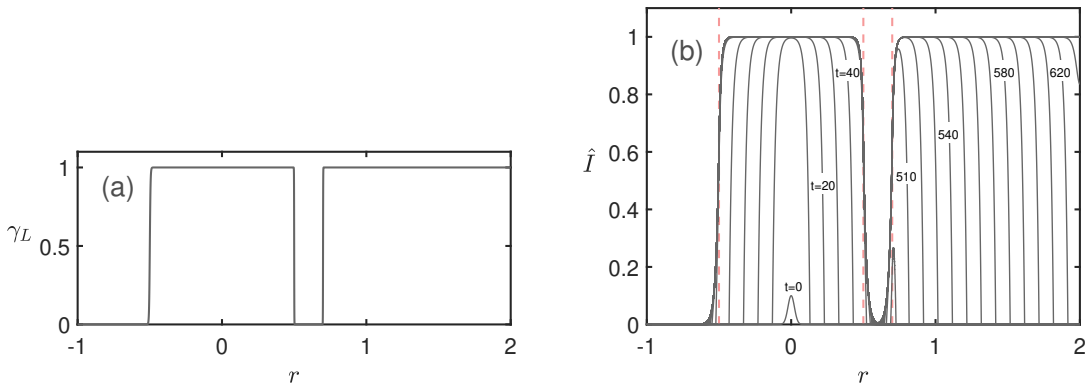

FIG. 3. (a) Linearly unstable region. (b) Evolution of equation (44) with $l_r = 10^{-2}$, the time interval between plot is 10.

and "Foot" in the unstable region, see figure 3(b). The front speed is well described by classic Fisher-KPP front speed, $V_f = \sqrt{2\gamma D}$ [11]. With the values $\gamma = 1$ and

$$D = \frac{1}{4} \times 2\hat{D}_0 = \frac{1}{2} l_{r*}^2 = \frac{1}{2} \times 10^{-4}$$

we have $V_f = 10^{-2}$. From equation above, we know as well, form the conventional spreading model, $V_f \propto l_{r*}$. This example sets the baseline for our study.

Solutions with $\delta_{b*} = 0.1$ are shown in figure 4. In figure 4(a), the convolution kernel in equation (46a) introduces a hyper-diffusion-like effect, which smooths the propagating front of $\langle \tilde{\phi}^2 \rangle$. Thus the distance between "Foot" and "Center" is greater in figure 4(a) than in figure 3. In figure 4 (b), which includes the nonlocal growth term (and corresponds to equation (46b)), the turbulence spreads faster and to a greater distance. The front width thickens and moves faster. The absolute depth of turbulence penetration is larger, than the curve in figure 4(a). When we fix the magnitude of l_r and vary δ_{b*}, one would expect that for larger δ_{b*}, the broader the leading edge and the deeper the penetration. If the box or unstable region is wide enough, there still exists a steady propagating front. The front propagation speed V_f should increase with δ_{b*}, too.

The fundamental effects of the nonlocal growth are easy to understand, since such a nonlocal growth term samples the growth rate from both the stable and unstable region. This increases the effective growth in the stable region and decreases the effective growth rate in the unstable region. When the width of the unstable region is small, as in the left unstable region in figure 4(b), this will affect the saturation level of turbulence, and therefore

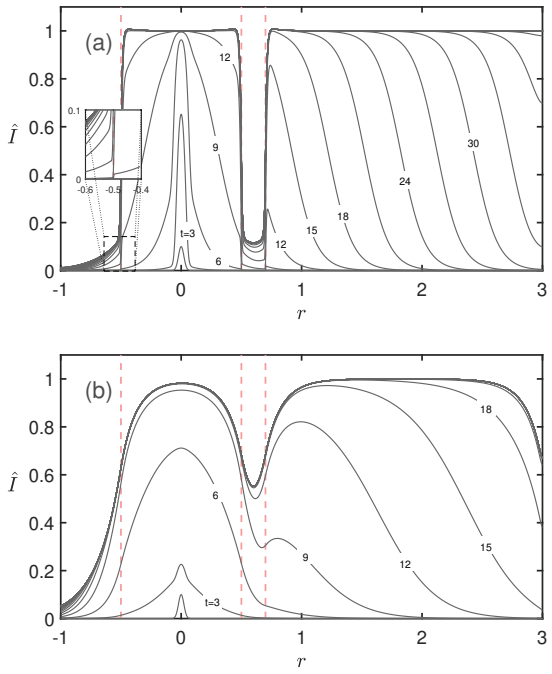

FIG. 4. Evolution of (a) equation (46a) (with nonlocal diffusion), (b) equation (46b) (with nonlocal growth). $l_r = \rho_* = 10^{-2}, \delta_{b*} = 10^{-1}$. The time interval for plotting is 3. Red vertical lines indicate the separatrix of linear growth region. The boundary conditions equation (49) successfully recover Neumann boundary in (a). Nonlocal growth term is not compatible with our boundary setting in (b). But as long as we set the boundary sufficiently far away from the evolving fronts, it won't affect the front propagation and penetration.

affect the transport scaling. However when the width of the unstable region is large enough to eliminate the sample from the stable region, as in the R.H.S. in figure 4(b), the saturation level will move back to 1, and the transport scaling should return to gyro-Bohm. Note that, when $\delta_{b*} = 0.1$, the small interval between the two unstable regions likely could not exist. Thus figure 4 is for demonstration.

To quantitatively understand the effects of nonlocal corrections to the models, we scanned the relation between both front speed V_{fr} and front shape for different values of δ_{b*}, at fixed l_{r*}. As we discussed in previous section, the control parameters are l_{r*} and the ratio between l_r and δ_{b*}. Results are as in figure 5 and figure 6. The range of δ_{b*} is from 0 to 0.1. We included the limit case where $\delta_{b*} < l_{r*}$ to illustrate the return to the prediction of the conventional model (equation (44)). All speeds and widths are calculated from fronts fully

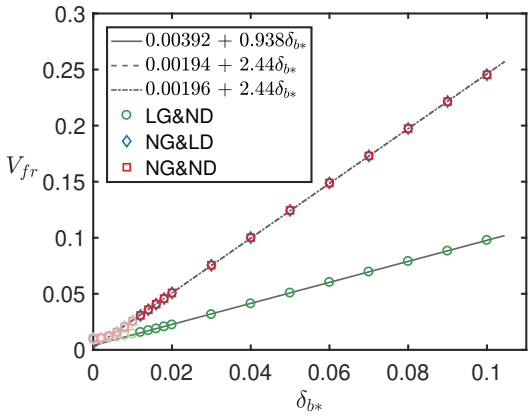

FIG. 5. Leading edge propagation speed for different models when varying δ_{b*} with $l_{r*} = 0.01$. Data points with lighter colors indicate where $\delta_{b*} < l_{r*}$, and are excluded from the fit lines. When $\delta_{b*} \to 0$, the speed converges to $\sqrt{2\gamma D} = 0.01$. Data form NG&ND and NG&LD overlapping indicates that the nonlocal growth effect dominates.

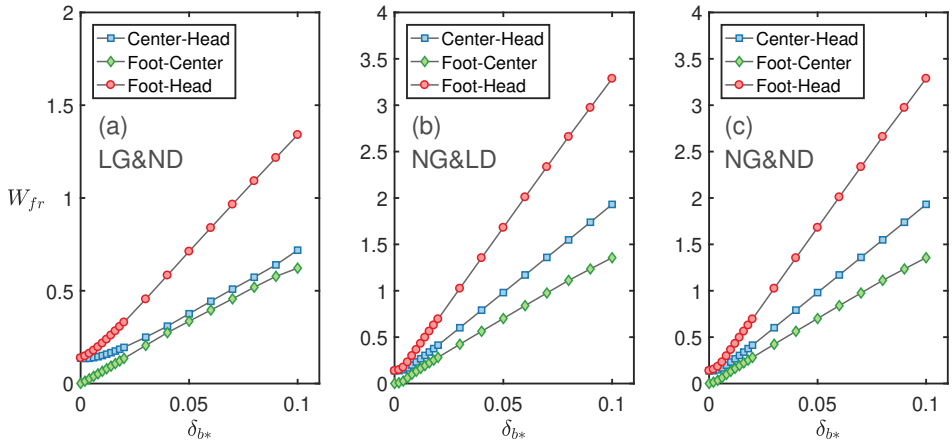

FIG. 6. Width of the propagating front in different equations with a fixed $l_{r*} = 10^{-2}$ when varying δ_{b*}. Nonlocal effects extend the front profiles with constant ratios to $\delta_{b}*$. The nonlocal models degenerate to the conventional local model as δ_{b*} decreases to 0. The difference between (b) and (c) is not distinguishable, which indicates that the nonlocal growth dominates.

saturated at 1, in a wide unstable region. So there is no size effect (L_T) in figure 5 and figure 6. We used NG for nonlocal growth and ND for nonlocal diffusion. So in figure 5 and 6, NG&ND represents for equation (45), LG&ND for (46a) and NG&LD for (46b).

The first feature we notice from figure 5 is that when δ_{b*} is larger than 0.01, the front

propagating speed increases approximately linearly with δ_{b*}. Fitting lines from equation (46b) and (45) with the nonlocal growth term show larger slopes than lines obtained from equation (46a), with local growth. When $\delta_{b*} < l_{r*}$ (the unphysical domain), the speed gradually transitions to the speed from the conventional model. So data points from $\delta_{b*} < l_{r*}$ are excluded from the fit. Notice we fixed l_r, so the speed varies only linearly with δ_{b*}. Another feature is the data points from NG&ND and NG&LD display almost no difference during the scan. So we conclude that the front speed is dominated by effects from nonlocal growth rather than nonlocal diffusion in equation (45). In other words, the effects of these two terms are not additive, and nonlocal growth is much more effective than nonlocal diffusion.

As for the front width, the thickness of the leading edges grow linearly with δ_{b*} as in figure 6. Notice that results from equation (45) and (46b) (i.e. NG&LD and NG&ND in figure 6) display almost the same behavior, except for tiny differences around $\delta_{b*} \sim 0.01$. This feature, together with the insensitivity of speed to nonlocal diffusion in the presence of nonlocal growth, suggests that our argument for the nonlocal extension of the coefficients is reasonable.

Furthermore, considering that equations (45) and (46b) both have nonlocal diffusion and differ only in the growth term, we can say that the nonlocal growth term is much more effective than nonlocal diffusion in intensity front generation. In other words, for intensity front propagation, we can neglect the nonlocal diffusion correction when there is nonlocal growth drive.

The most important aspect of turbulence spreading is to understand to what extent turbulence extends into the stable region. In our numerical studies, the penetration depth Δ_p is defined by where the front foot start to exceed 10^{-2} of the saturation level. In figure 7, after the front crosses the separatrix, Δ_p increases quickly in a relatively short time, then slowly penetrates to a relatively stable depth. The shape of penetration front could be different for the cases with only nonlocal diffusion. Specifically, in figure 7(a), the intensity around the separatrix ($r \approx 0.5$) decreases with δ_{b*}, but then increases for $r \gtrsim 0.6$. Though this difference might be tiny, we would like to introduce the areas covered by the profile in the stable region S_p to characterize the effective penetration depth (see definition in figure 2). In figure 8, we scan Δ_p and S_p for different equations by varying δ_{b*}. Both Δ_p and S_p can be well fit in the line of $C\delta_{b*}$ with a constant C, when $\delta_{b*} > l_{r*}$. Therefore, we have the

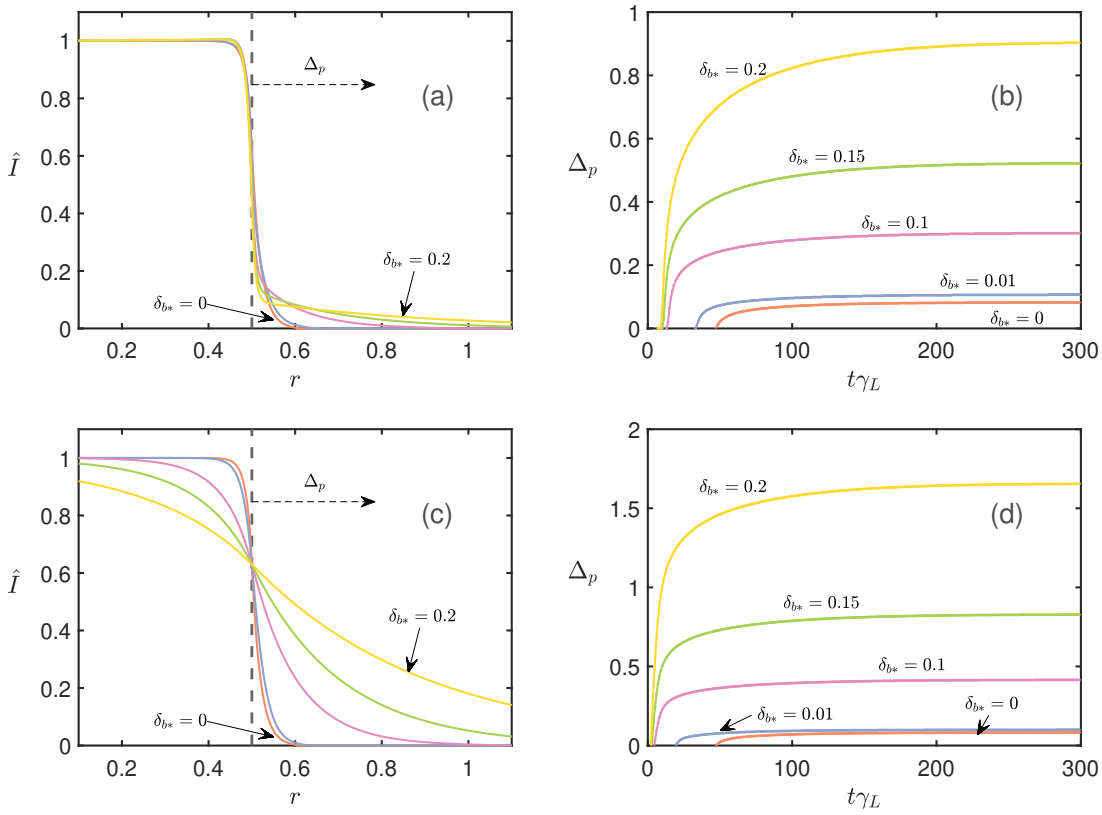

FIG. 7. Leading edge penetrates into unstable region. (a) and (b) correspond to equation (46a) with nonlocal diffusion. (c) and (d) correspond to equation (46b) with nonlocal growth. δ_{b*} varies in range (0, 0.01, 0.1, 0.15, 0.2). (a) and (c) are plotted at $t\gamma_L = 300$.

conclusion:

$$\Delta_p, S_p \propto \delta_{b*} \tag{50}$$

The message is quite simple and clear: *Nonlocal effects enhance the spreading into stable region.* The larger the range of the nonlocal kernel, the deeper the spreading occurs. Notice that data points from NG&ND overlap with from NG&LD. This indicates that the nonlocal growth effect again dominates. When we compare figure 8(a) and (b), we notice that the effective penetration S_p from nonlocal diffusion is small compared to those from nonlocal growth, even though the Δ_p values have similar magnitudes. The remain fraction of turbulence in the unstable region, when summed up as $\bar{\hat{I}} \equiv \int \hat{I} \mathrm{d}r / L_T$, follows a simple linear relation with δ_{b*}:

$$\bar{\hat{I}} = \bar{I}/l_{r*}^2 = 1 - \delta_{b*} \tag{51}$$

The transport coefficient scales in the same way, since $D(I) = D_0 I$. This could be a

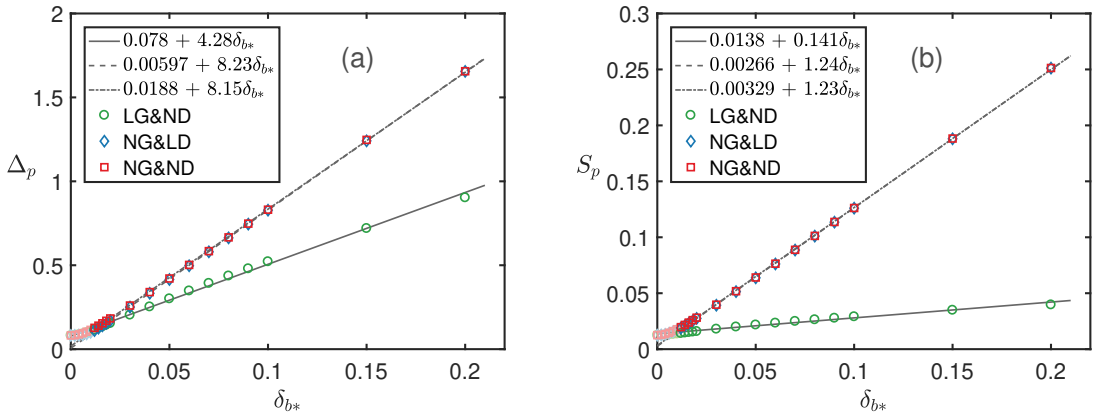

FIG. 8. Front penetration Δ_p (a) and effective penetration S_p (b) against δ_{b*} for different equations. All curve are plotted at $t\gamma_L = 300$. Simple linear relation can fit both Δ_p and S_p, when $\delta_{b*} > l_{r*}$. Data points in lighter colors are excluded from the fits.

supplement to the interpretation of varies gyro-kinetic simulations [10, 28, 29, 31].

V. DISCUSSION AND CONCLUSIONS

In this paper, we have developed a theory of turbulence spreading for the Darmet et al. model [17–19] of trapped ion drift wave fluctuations. The theory demonstrates that the evolution of the potential fluctuation intensity is explicitly nonlocal. The principal results of this paper are:

1. The derivation of an evolution equation for the two point correlation function of potential vorticity.

2. The closure of this equation, using a two-point quasilinear method. The result is specialized to the case of interest - namely turbulence spreading. Thus, we focus on evolution of the two particles centroid in r, and on the relative coordinates in $\theta \rightarrow$ here y_-. The equation be derived contains all the basic effects considered in heuristic $K - \varepsilon$ models.

3. The derivation of an intensity evolution equation, obtained by inverting PV to electric potential. The intensity equation has the structure of a delocalized nonlinear Fisher

equation [32, 33], of schematic form (after equation (43)):

$$\partial_t \left\langle \tilde{\phi}^2 \right\rangle = \mathcal{G} \otimes [\text{Nonlinear Diffusion}] + \mathcal{G} \otimes \left(\gamma_L(r) \left\langle \tilde{\phi}^2 \right\rangle \right) - \frac{D_0}{l_r^2} \left\langle \tilde{\phi}^2 \right\rangle^2$$

Here $\mathcal{G}$ is a Green's function and $\otimes$ refers to a spatial convolution,

4. The important observation is that the intensity equation is explicitly non-local, with a range of non-locality set by $\mathcal{G}$. Note that in general, *the scale of PV inversion sets the range of the explicit nonlocality.* Here this length scale is δ_b, which is modest.

5. The determination that the explicit non-local growth is the principal new effect.

6. The observation that the nonlocal growth enhances the speed of intensity front propagation ($V \simeq (\gamma D)^{1/2}(1+\delta_b)$) and the depth of penetration into the stable region by a front originating in the unstable region. This penetration depth scales as $\Delta_p \sim \delta_{b*}$.

7. The result that enhanced turbulence spreading effects tend to lower average saturated levels in the unstable region. If the unstable region is spatially symmetric, saturation level scales according to $\bar{\hat{I}} = 1 - \delta_{b*}$.

More generally, the paper once again demonstrates the utility of PV (potential vorticity), and that turbulence spreading is best formulated in terms of this conserved (or conserved up to linear effects) quantity. It also shows that the potential enstrophy evolution equation is the optimal way to address and calculate intensity spreading. This work also identifies that there indeed exists an explicit non-locality, which arises as a consequence of PV inversion. The range of this non-locality is the range of the PV inversion kernel. A good question is what nonlocal physics could be missed in equation (39), comparing to equation (27). Actually, the nonlocality is implicitly buried in the triplet terms, for example $\langle \tilde{v}_{r_1} \widetilde{U_1 U_2} \rangle$, in equation (27), since $\tilde{\phi}$ has a nonlocal relation with the quantity $\tilde{U}$ (the PV) described in this equation. The inversion of $\tilde{U}$ to $\tilde{\phi}$ make the nonlocality explicit. Some nonlocality scattering effects could be truncated because of the 2-point quasilinear approximation.

In the relevant case of trapped ion mode fluctuations, we note that the scale of explicit nonlocality in radial direction is δ_b, and so such effects here are modest. This is in accord with the conventional wisdom that while transport dynamics are nonlocal, they are only

weakly so. However, this theory determines systematically the scale of such effects, on the basis of fundamental physics. Also, we note that near conditions of macroscopic marginality, where the range of the PV inversion can become long, so can the range of explicit nonlocality. Or any other mechanism of which enhances the scale of the screening response could enhance the nonlocality, and therefore results in a nonlocal transport beyond modest.

We should add, however, that "weakly nonlocal" is quite different from "quasilinear". The physics content of the turbulence intensity evolution equation is important and essential. The impact of intensity field explicit nonlocality can be substantial. C. Gillot [34] told , intensity evolution is an important component of a transport model.

Regarding future directions, one obvious suggestion is application to energetic particle-driven turbulence, especially EPM fluctuations [35, 36]. There, the scale δ_b can be large, so explicit nonlocality effects can be *much* stronger. Cross-scale coupling can affect the bulk transport, as well. Another direction is toward pedestal turbulence, where δ_b/L_T is not so small. Indeed, pedestal nonlocality may be a simplifying effect, as it will wash out the microstructure which is frequently discussed [37]. We also aim to include zonal flows in the analysis. Note that propagating turbulence can be expected to simply drag the zonal model along with it, since the former generates the latter. Less clear, however, is what happens when zonal mode friction varies in space, leading to transitions, say, between Dimits-shift-like and heavily damped regimes. Finally, we hope to dispense with $\langle\tilde{\phi}\tilde{\phi}\rangle$, and to calculate directly the evolution of the flux, i.e. to obtain an equation of the form $\partial_t\langle\tilde{v}_r\tilde{T}\rangle = \cdots$. This result will then be applied to the evolution of staircase formation, via jamming [38, 39]. These extensions will be discussed in future works.

Appendix A: Expansion Approximation of Convolution

The convolution form will keep the values positive as long as the intensity is positive at the beginning. But approximating the convolution with higher-order derivatives can result in negative values of intensity. A simple linear analysis of equation (43) shows why. Think of the convolution as an operator:

$$\left(\int_0^\infty e^{-|r|/\delta_b}\right) \otimes \Rightarrow 1 + \delta_b^2\partial_r^2 + \delta_b^4\partial_r^4 + \cdots \Rightarrow 1 - \delta_b^2 m_r^2 + \delta_b^4 m_r^4 - \cdots \tag{A1}$$

Here we use m_r to represent the mode number of $\langle\tilde{\phi}^2\rangle$, so as to make a distinction with the mode number k of $\tilde{\phi}$. Then equation (43) can be written as:

$$-i\omega\langle\tilde{\phi}^2\rangle_{m_r} = \left(1-\delta_b^2 m_r^2+\delta_b^4 m_r^4-\cdots\right)\left(\gamma_L\langle\tilde{\phi}^2\rangle_{m_r}-2D_0 m_r^2(1+\frac{\delta_b^2}{2}m_r^2)\langle\tilde{\phi}^2\rangle^2_{m_r}\right)-\frac{D_0}{l_r^2}\langle\tilde{\phi}^2\rangle^2_{m_r} \tag{A2}$$

Let $\omega=\omega_R+i\gamma_{\rm total}$, which contains the real part and total growth rate. Because $m_r\sim l_s^{-1}$ and $l_s>\delta_b$, we can try to approximate the convolution to different order of $\delta_b^2 m_r^2$. For example, zero-th order of approximation leads to

$$\gamma^{(0)}_{\rm total}=\gamma_L-\left(2D_0 m_r^2+\frac{D_0}{l_r^2}\right)\langle\tilde{\phi}^2\rangle_{m_r} \tag{A3}$$

This corresponds to the usual turbulence spreading model. The evolution of $\langle\tilde{\phi}^2\rangle$ is excited by linear growth γ_L and saturates for a large enough positive value of $\langle\tilde{\phi}^2\rangle$. If we include the next order (second order) approximation, we obtain,

$$\gamma^{(0)}_{\rm total}+\gamma^{(2)}_{\rm total}=\gamma_L-\left(2D_0 m_r^2+\frac{D_0}{l_r^2}\right)\langle\tilde{\phi}^2\rangle_{m_r}-\delta_b^2 m_r^2\gamma_L+\delta_b^2 D_0 m_r^4\langle\tilde{\phi}^2\rangle_{m_r} \tag{A4}$$

The third term of R.H.S. of equation above comes from the approximation of the convolution with growth rate and does no harm to the saturation. But the forth term in R.H.S of above equation can break the saturation mechanism when m_r is big enough for a positive $\langle\tilde{\phi}^2\rangle_{m_r}$. And a negative $\langle\tilde{\phi}^2\rangle_{m_r}$ can still saturate, therefore in the evolution of $\langle\tilde{\phi}^2\rangle$ can have negative values. When we continue to include the forth order approximation, we obtain,

$$\gamma^{(4)}_{\rm total}=\delta_b^4 m_r^4\gamma_L-\delta_b^4 D_0 m_r^6\langle\tilde{\phi}^2\rangle_{m_r} \tag{A5}$$

It seems eliminate the high m_r problems but now requires a 6th order derivative and a finer mesh gird. A brief conclusion is the negative value of intensity is caused by the nonlocal nonlinear diffusion term in equation (43). As we showed in the paper it can be simplified as the usual nonlinear diffusion as long as the nonlocal growth exists. Such behavior is a result of the factor 1/2 in $2D_0 m_r^2(1+\frac{\delta_b^2}{2}m_r^2)\langle\tilde{\phi}^2\rangle^2_{m_r}$, which appears because we persist in the sequency of doing the integral first, then taking the limitation $1\to 2$. So it is not crucial for the physics.

ACKNOWLEDGMENTS

We thank the help discussion with T S Hahm, X Garbet, G Dif-Pradalier, Z B Guo, Zhe Gao and Min Xu. We thank participants in the 2018 Chengdu Theory Festival, the 2019

Festival de Théorie and the 2021 KITP program "staircase 21" for stimulating discussions. This work is supported by National Key R&D Program of China under 2017YFE0301201, National Natural Science Foundation of China under Grant Nos. 11875124, 11705052, 11905050, U1867222 and 11875023, and Science and Technology Department of Sichuan Province under Grant No. 2020JDTD0030. The work is also supported by the U.S. Department of Energy, Office of Science, Office of Fusion Energy Sciences under Award Number DE-FG02-04ER54738 and by the U.S. Natl. Sci. Foundation under Grant No. PHY-1748958.

REFERENCES

[1] F Wagner. A quarter-century of H-mode studies. *Plasma Phys. Control. Fusion*, 49(12B):B1–B33, December 2007.

[2] B B Kadomtsev. Plasma turbulence. *New York: Academic Press*, 1965.

[3] P H Diamond, S I Itoh, K Itoh, and T S Hahm. Zonal flows in plasma - a review. *Plasma Phys. Control. Fusion*, 47(5):R35–R161, 2005.

[4] G R McKee, C C Petty, R E Waltz, C Fenzi, R J Fonck, J E Kinsey, T C Luce, K H Burrell, D R Baker, E J Doyle, X Garbet, R A Moyer, C L Rettig, T L Rhodes, D W Ross, G M Staebler, R Sydora, and M R Wade. Non-dimensional scaling of turbulence characteristics and turbulent diffusivity. *Nucl. Fusion*, 41(9):1235–1242, 2001.

[5] R V Budny, D R Ernst, T S Hahm, D C McCune, J P Christiansen, J G Cordey, C G Gowers, K Guenther, N Hawkes, O N Jarvis, P M Stubberfield, K D Zastrow, L D Horton, G Saibene, R Sartori, K Thomsen, and M G von Hellermann. Local transport in joint European Tokamak edge-localized, high-confinement mode plasmas with H, D, DT, and T isotopes. *Phys. Plasmas*, 7(12):5038–5050, 2000.

[6] K Ida, Z Shi, H J Sun, S Inagaki, K Kamiya, J E Rice, N Tamura, P H Diamond, G Dif-Pradalier, X L Zou, K Itoh, S Sugita, Ö D Gürcan, T Estrada, C Hidalgo, T S Hahm, A Field, X T Ding, Y Sakamoto, S Oldenbürger, M Yoshinuma, T Kobayashi, M Jiang, S H Hahn, Y M Jeon, S H Hong, Y Kosuga, J Dong, and S-I Itoh. Towards an emerging understanding of non-locality phenomena and non-local transport. *Nucl. Fusion*, 55(1):013022, January 2015. Publisher: IOP Publishing.

[7] K W Gentle, R V Bravenec, G Cima, H Gasquet, G A Hallock, P E Phillips, D W Ross, W L Rowan, A J Wootton, T P Crowley, J Heard, A Ouroua, P M Schoch, and C Watts. An experimental counter-example to the local transport paradigm. *Phys. Plasmas*, 2(6):2292–2298, June 1995.

[8] Y J Shi, Z J Yang, Z Y Chen, Z F Cheng, X Y Zhang, W Yan, J Wen, Q X Cai, K J Zhao, S C Hong, J M Kwon, P H Diamond, P Shi, H Zhou, X M Pan, Z P Chen, S M Yang, Y B Dong, L Wang, Y H Ding, Y F Liang, Z B Shi, Y-S Na, and the J-TEXT team. Observation of non-local effects in ion transport channel in J-TEXT plasmas. *Nucl. Fusion*, 60(6):064002, June 2020.

[9] X Garbet, L Laurent, A Samain, and J Chinardet. Radial propagation of turbulence in tokamaks. *Nucl. Fusion*, 34(7):963–974, 1994.

[10] T S Hahm, P H Diamond, Z Lin, K Itoh, and S-I Itoh. Turbulence spreading into the linearly stable zone and transport scaling. *Plasma Phys. Control. Fusion*, 46(5A):A323–A333, 2004.

[11] Ö D Gürcan, P H Diamond, T S Hahm, and Z Lin. Dynamics of turbulence spreading in magnetically confined plasmas. *Phys. Plasmas*, 12(3):032303, 2005.

[12] P H Diamond and T S Hahm. On the dynamics of turbulent transport near marginal stability. *Phys. Plasmas*, 2(10):3640–3649, October 1995. Publisher: American Institute of Physics.

[13] P H Diamond, S Champeaux, M Malkov, A Das, I Gruzinov, M N Rosenbluth, C Holland, B Wecht, A I Smolyakov, F L Hinton, Z Lin, and T S Hahm. Secondary instability in drift wave turbulence as a mechanism for zonal flow and avalanche formation. *Nucl. Fusion*, 41(8):1067–1080, August 2001.

[14] T S Hahm and P H Diamond. Mesoscopic transport events and the breakdown of Fick's law for turbulent fluxes. *J. Korean Phys. Soc.*, 73(6):747–792, September 2018.

[15] G Dif-Pradalier, V Grandgirard, Y Sarazin, X Garbet, and Ph Ghendrih. Interplay between Gyrokinetic Turbulence, Flows, and Collisions: Perspectives on Transport and Poloidal Rotation. *Phys. Rev. Lett.*, 103(6):065002, August 2009. Publisher: American Physical Society.

[16] G Dif-Pradalier, P H Diamond, V Grandgirard, Y Sarazin, J Abiteboul, X Garbet, Ph Ghendrih, A Strugarek, S Ku, and C S Chang. On the validity of the local diffusive paradigm in turbulent plasma transport. *Phys. Rev. E*, 82(2):025401, August 2010.

[17] G Depret, X Garbet, P Bertrand, and A Ghizzo. Trapped ion driven turbulence in tokamak plasmas. *Plasma Phys. Control. Fusion*, 42(9):949–971, September 2000.

[18] Y Sarazin, V Grandgirard, E Fleurence, X Garbet, Ph Ghendrih, P Bertrand, and G Depret. Kinetic features of interchange turbulence. *Plasma Phys. Control. Fusion*, 47(10):1817–1839, October 2005.

[19] G Darmet, Ph Ghendrih, Y Sarazin, X Garbet, and V Grandgirard. Intermittency in flux driven kinetic simulations of trapped ion turbulence. *Communications in Nonlinear Science and Numerical Simulation*, 13(1):53–58, February 2008.

[20] M N Rosenbluth and F L Hinton. Poloidal Flow Driven by Ion-Temperature-Gradient Turbulence in Tokamaks. *Phys. Rev. Lett.*, 80(4):724–727, January 1998. Publisher: American Physical Society.

[21] L Chen, Z Lin, and R White. Excitation of zonal flow by drift waves in toroidal plasmas. *Phys. Plasmas*, 7(8):3129–3132, July 2000.

[22] W Dorland and G W Hammett. Gyrofluid turbulence models with kinetic effects. *Physics of Fluids B: Plasma Physics*, 5(3):812–835, March 1993.

[23] P N Guzdar, R G Kleva, and L Chen. Shear flow generation by drift waves revisited. *Phys. Plasmas*, 8(2):459–462, February 2001.

[24] T H Dupree. Theory of phase space density granulation in plasma. *Phys. Fluids*, 15(2):334, 1972.

[25] P H Diamond, S-I Itoh, and K Itoh. *Modern Plasma Physics*, volume 1. Cambridge University Press, 2010.

[26] Ö D Gürcan, P H Diamond, and T S Hahm. Radial transport of fluctuation energy in a two-field model of drift-wave turbulence. *Phys. Plasmas*, 13(5):052306, May 2006.

[27] P Migliano, R Buchholz, S R Grosshauser, W A Hornsby, and A G Peeters. The radial propagation of turbulence in gyro-kinetic toroidal systems. *Plasma Phys. Control. Fusion*, 57(5):054008, April 2015.

[28] Z Lin, S Ethier, T S Hahm, and W M Tang. Size scaling of turbulent transport in magnetically confined plasmas. *Phys. Rev. Lett.*, 88(19):195004, May 2002.

[29] B F McMillan, X Lapillonne, S Brunner, L Villard, S Jolliet, A Bottino, T Goerler, and F Jenko. System size effects on gyrokinetic turbulence. *Phys. Rev. Lett.*, 105(15):155001, October 2010.

[30] K Miyamoto. *Plasma Physics and Controlled Nuclear Fusion*. Springer-Verlag, 2005.

[31] R E Waltz and J Candy. Heuristic theory of nonlocally broken gyro-Bohm scaling. *Phys. Plasmas*, 12(7):072303, 2005.

[32] R A Fisher. The wave of advance of advantageous genes. *Annals of Eugenics*, 7(4):355–369, June 1937. Publisher: John Wiley & Sons, Ltd.

[33] A N Kolmogorov, I G Petrovskii, and N S Piskunov. *A Study of the Diffusion Equation with Increase in the Amount of Substance, and Its Application to a Biological Problem in Selected Works of AN Kolmogorov, vol. 1, 242-270*. London: Kluwer Academic Publishers (Appeared in Bull. Moscow Univ., Math. Mech. 1: 6 ….

[34] C Gillot and et al. Submitted to Phys. Rev. Lett. 2021.

[35] Liu Chen. Theory of magnetohydrodynamic instabilities excited by energetic particles in tokamaks*. *Physics of Plasmas*, 1(5):1519–1522, May 1994. Publisher: American Institute of Physics.

[36] F Zonca, S Briguglio, L Chen, G Fogaccia, and G Vlad. Transition from weak to strong energetic ion transport in burning plasmas. *Nucl. Fusion*, 45(6):477–484, May 2005. Publisher: IOP Publishing.

[37] R J Groebner, C S Chang, J W Hughes, R Maingi, P B Snyder, X Q Xu, J. A. Boedo, D. P. Boyle, J. D. Callen, J. M. Canik, I. Cziegler, E. M. Davis, A. Diallo, P. H. Diamond, J. D. Elder, D. P. Eldon, D. R. Ernst, D. P. Fulton, M. Landreman, A. W. Leonard, J. D. Lore, T. H. Osborne, A. Y. Pankin, S. E. Parker, T. L. Rhodes, S. P. Smith, A. C. Sontag, W. M. Stacey, J. Walk, W. Wan, E. H.-J. Wang, J. G. Watkins, A. E. White, D. G. Whyte, Z. Yan, E. A. Belli, B. D. Bray, J. Candy, R. M. Churchill, T. M. Deterly, E. J. Doyle, M. E. Fenstermacher, N. M. Ferraro, A. E. Hubbard, I. Joseph, J. E. Kinsey, B. LaBombard, C. J. Lasnier, Z. Lin, B. L. Lipschultz, C. Liu, Y. Ma, G. R. McKee, D. M. Ponce, J. C. Rost, L. Schmitz, G. M. Staebler, L. E. Sugiyama, J. L. Terry, M. V. Umansky, R. E. Waltz, S. M. Wolfe, L. Zeng, and S J Zweben. Improved understanding of physics processes in pedestal structure, leading to improved predictive capability for ITER. *Nucl. Fusion*, 53(9):093024, August 2013. Publisher: IOP Publishing.

[38] Y Kosuga, P H Diamond, and Ö D Gürcan. How the Propagation of Heat-Flux Modulations Triggers E x B Flow Pattern Formation. *Phys. Rev. Lett.*, 110(10):105002, March 2013.

[39] Y Kosuga, P H Diamond, G Dif-Pradalier, and Ö D Gürcan. E×B shear pattern formation by radial propagation of heat flux waves. *Phys. Plasmas*, 21(5):055701, May 2014.